BIOCH 590: Biomacromolecules Spring 2010

Nuclear Magnetic Resonance

Basic Principles and Applications to Biomolecules

Key References: Tinoco Chapter 10; van Holde Chapter 12;

Overview

- Basic principles
  - Nuclear spin, energy levels, chemical shift
  - Through-bond and through space couplings
  - Relaxation times
  - FT-NMR, pulses, 1D NMR
  - 2D and multi-dimensional NMR experiments
- Application to biomolecules
  - High-resolution structure determination
  - Dynamics: relaxation analysis
  - Transient interactions: excitation transfer, spin-labeling
  - Solid state: membrane proteins
  - In-cell NMR
  - Imaging: MRI

NMR Fundamentals

Nuclear Spin

- Spin: fundamental property of elementary particles
  - Electron: S = ½
- Nucleus: consist of protons and neutrons
  - (Net) nucleus spin number: *I* = 0, ½, 1, …
  - No nucleus spin if even numbers of neutrons *and* protons

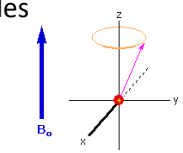

Isotope	Spin	γ (Gyromag. Rat) (10^7 rad/sec T)	Natural abundance (%)	Relative Sensitivity	ν/MHz at 11.7 T field
^1H	½	26.7522	99.98	1.00	500.0
^2H	1	4.1066	0.015	9.65×10^{-3}	76.8
^{13}C	½	6.7283	1.108	1.59×10^{-2}	125.8
^{15}N	½	-2.7126	0.37	1.04×10^{-3}	50.6
^{19}F	½	25.1815	100	0.83	470.6
^{31}P	½	0.8394	100	6.63×10^{-2}	202.6

Energy Levels

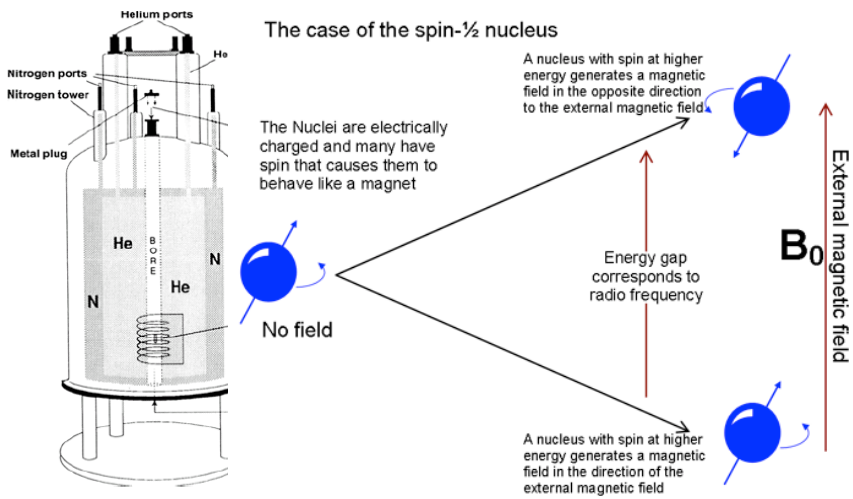

- NMR mostly concerns ½ nuclei: ^{1}H, ^{13}C, ^{15}N etc

Energy Levels

- Magnetic dipole

$$\mu_z = \gamma\hbar m_z$$

  - γ: Gyromagnetic ratio
- Energy levels

$$E = -\mu_z B_0 = -\gamma\hbar m_z B_0$$

- Energy gap

$$\Delta E = \gamma\hbar B_0 = h\nu_L$$

  - Larmor frequency: $\upsilon_L = \gamma B_0/2\pi$
  - Strength of magnetic field determines the energy gap of a given nuclei.

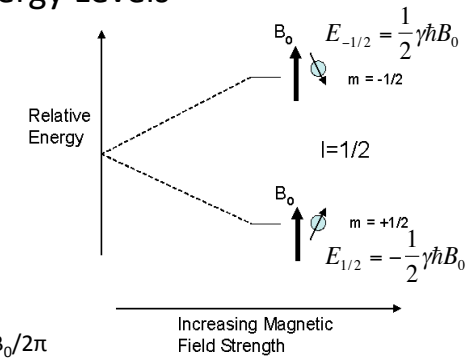

IR probes vibrational energy levels with energy gaps ~ 6 kcal/mol.
On a typical NMR spectrometer, the NMR energy gap is ~ 10^{-5} kcal/mol.

Higher magnetic field: increase spectral width and resolution
enhance spectral sensitivity

Magnet Strength and Proton Frequency

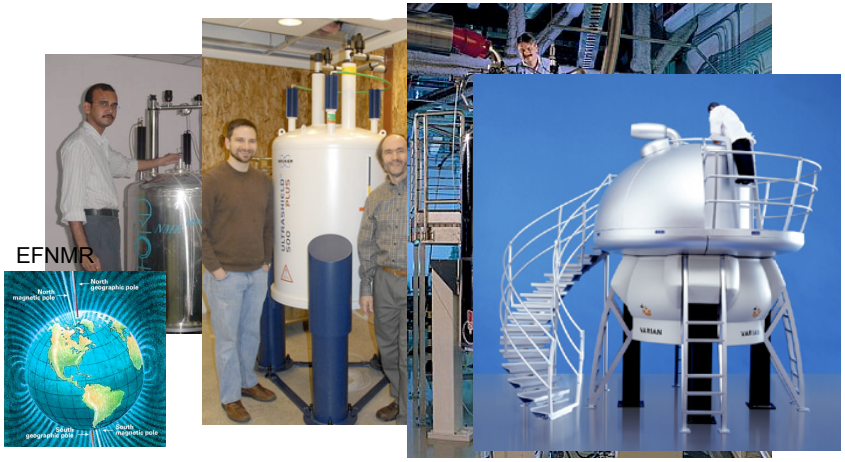

~10^{-5} T	1.41 T	11.75 T	18.8 T	21.15 T
~ KHz	60 MHz	500 MHz	800 MHz	900 MHz
$0		$0.5m		>$5m

NMR Spectrum

Absorption when radiation matches the energy gap

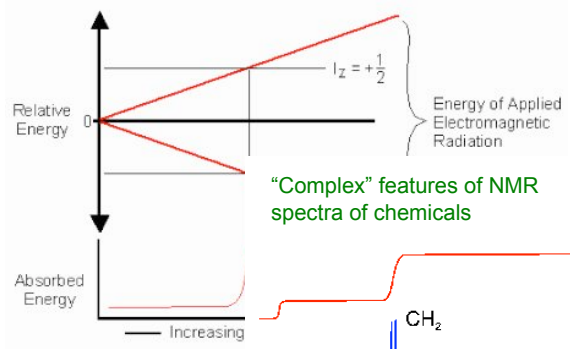

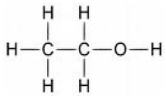

"Complex" features of NMR spectra of chemicals

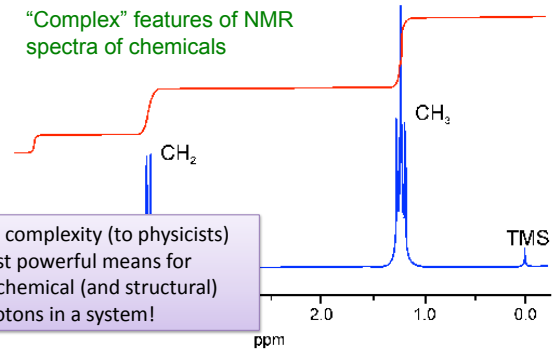

Such initially unpleasant complexity (to physicists) becomes one of the most powerful means for chemists to probe local chemical (and structural) environments of (all) protons in a system!

Chemical Shift

- Local variations of magnetic field

$$\upsilon_s = \upsilon_0(1-\sigma)$$

  - σ: shielding coefficient
- Chemical shift

$$\delta_s = \frac{\upsilon_s - \upsilon_{ref}}{\upsilon_0} \cong \frac{\upsilon_s - \upsilon_{ref}}{\upsilon_{ref}}$$

  - Expressed in ppm
  - Reference standard: tetramethylsilane (TMS) (or DDS)
    - Singlet: all 12 protons NMR equivalent
    - TMS is very shielded and resonate at high requency
    - Most compounds studied by ^{1}H NMR absorb downfield of the TMS signal, thus there is usually no interference between the standard and the sample.

Figure 2. Creation of the B_e field by the circulation of electrons in response to the B_o field. B_e opposes B_o at the nucleus.

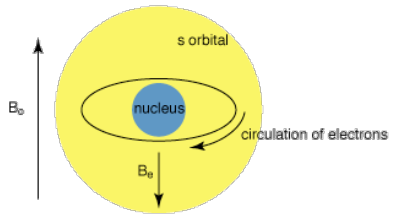

B_e opposes B_o and shields the nucleus from the effect of B_o

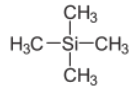

A few confusing terminologies

- Downfield (high ppm) vs. upfield (low ppm)
- High frequency (high ppm) vs low frequency (low ppm)

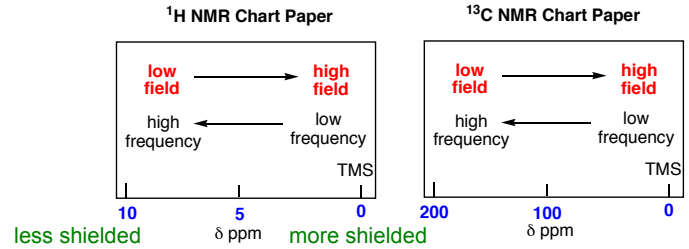

Nuclei which absorb at higher field are more shielded from the applied B_o field by their respective B_e fields. For these nuclei (B_o-B_e) is smaller and correspondingly a lower frequency ν is required to achieve resonance.

http://orgchem.colorado.edu/hndbksupport/nmrtheory/chemshift.html

Typical Chemical Shifts

- Local shielding: higher electron density -> more shielding
  - Electronegative substituents withdraw electron and thus reduce shielding
- Interatomic shielding and ring currents
  - Induced magnetic field might oppose or enhance external magnetic field!

$$\upsilon_s = \upsilon_0(1-\sigma)$$

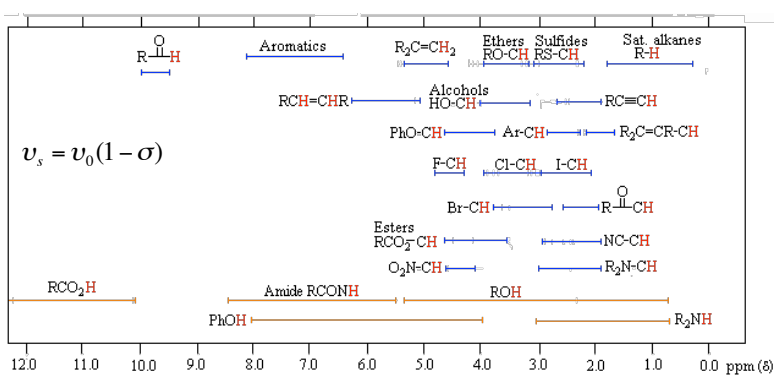

Why do different protons absorb at different frequencies of the B_1 field?

Electronegative elements such as oxygen pull electron density away from the hydrogen nucleus.

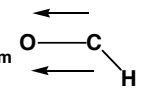

This decreases the magnitude of the shielding B_e field and **increases** (B_o-B_e).

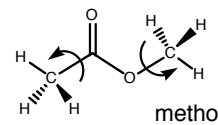

methyl acetate

methyl δ=2.1 ppm

methoxy δ=3.7 ppm

Circulation of π electrons creates magnetic fields which contribute to the B_e field. The contribuiton is a function of orientation and consequently is an anisotropic effect.

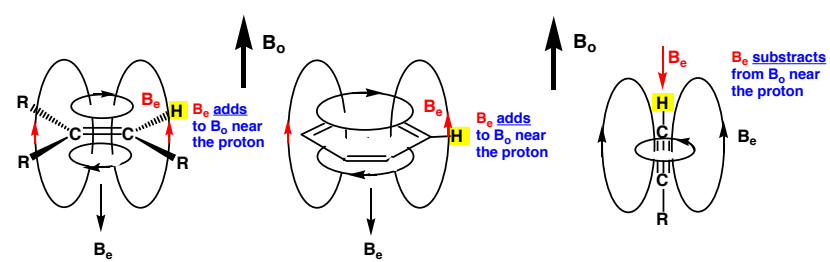

http://orgchem.colorado.edu/hndbksupport/nmrtheory/chemshift.html

Approximate Chemical Shifts

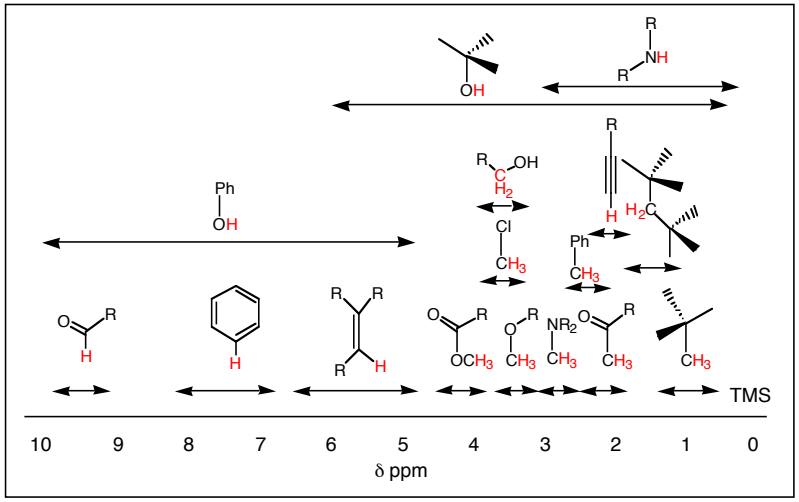

http://orgchem.colorado.edu/hndbksupport/nmrtheory/chemshift.html

Chemical Shift Indexing

- Chemical shifts further depend on (local) structures
  - For example, −0.35 ppm, on average, for Hα in helices, and +0.40 ppm, on average, for Hα in β-sheets (Jimenez et al. 1987)
- CSI: a powerful mean for obtaining protein secondary structures
  - Compared to random coil reference values

Residue	^{1}Hα ± 0.1 ppm	^{13}Cα ± 0.7 ppm	^{13}Cβ ± 0.7 ppm	^{13}C′ ± 0.5 ppm
Ala	4.4	52.5	19.0	177.1
Cys(red)	4.7	58.8	28.6	174.8
CYS(ox)		58.0	41.8	175.1

  - averages assignments from multiple chemical shifts (^{1}Hα, ^{13}Cα, ^{13}Cβ and ^{13}C′) to arrive at a consensus assignment.

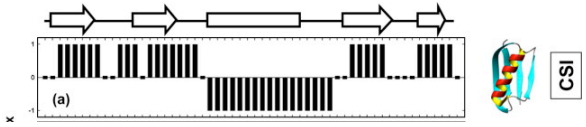

- Latest extensions to reliable tertiary structure determination by combining CS and statistical knowledge! (e.g., see Bax PNAS 2008)

Mielke and Krishnan, Prog. NMR Spect (2009)

NMR Peak Intensity

- The magnitude or intensity of NMR resonance is proportional to the molar concentration of the sample, which is most accurately measured as integrated intensity (commonly displayed on 1D NMR spectra)
- Integrated intensity is proportional to number of protons

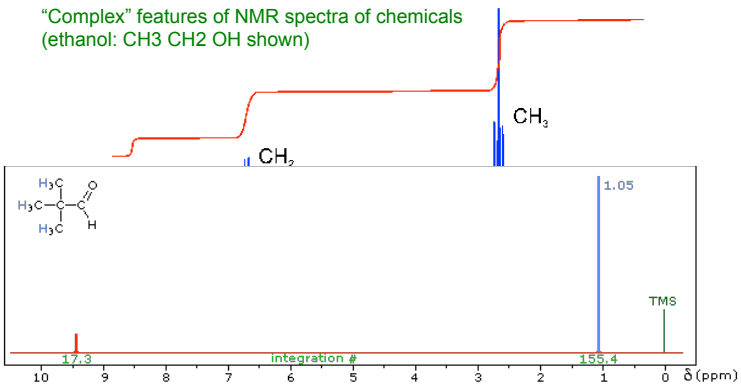

Spin-Spin Coupling

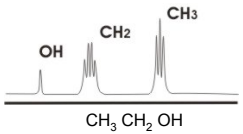

- A.k.a. Scalar coupling (J-coupling)
- Between NMR non-equivalent nuclei
  - Different chemical shifts
  - Different chemical environment and not enantiomeric pairs
- Through chemical bonds (electron spin)
  - Deceases with more bonds: no more than four bonds
  - J ~ 0 - 20 Hz (depends on chemical nature and structure)
  - J (measured in Hz) is field strength independent!
- Leads to splitting of the magnetic spin energy levels, thus, signals
  - In the limit of J << chemical shift difference (first order/weak coupling)
  - Split into N+1 peaks if coupled to N adjacent equivalent protons
  - The intensities of these peaks follow Pascal's triangle

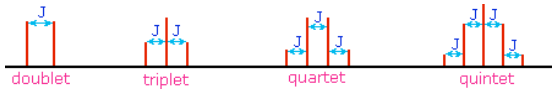

1
1 1
1 2 1
1 3 3 1
1 4 6 4 1

Energy Levels and J-Coupling

number	spin states	energy
1	$\alpha\alpha$	$+\frac{1}{2}\nu_{0,1} + \frac{1}{2}\nu_{0,2} + \frac{1}{4}J_{12}$
2	$\alpha\beta$	$+\frac{1}{2}\nu_{0,1} - \frac{1}{2}\nu_{0,2} - \frac{1}{4}J_{12}$
3	$\beta\alpha$	$-\frac{1}{2}\nu_{0,1} + \frac{1}{2}\nu_{0,2} - \frac{1}{4}J_{12}$
4	$\beta\beta$	$-\frac{1}{2}\nu_{0,1} - \frac{1}{2}\nu_{0,2} + \frac{1}{4}J_{12}$

transition	spin states	frequency
$1 \to 2$	$\alpha\alpha \to \alpha\beta$	$-\nu_{0,2} - \frac{1}{2}J_{12}$
$3 \to 4$	$\beta\alpha \to \beta\beta$	$-\nu_{0,2} + \frac{1}{2}J_{12}$
$1 \to 3$	$\alpha\alpha \to \beta\alpha$	$-\nu_{0,1} - \frac{1}{2}J_{12}$
$2 \to 4$	$\alpha\beta \to \beta\beta$	$-\nu_{0,1} + \frac{1}{2}J_{12}$

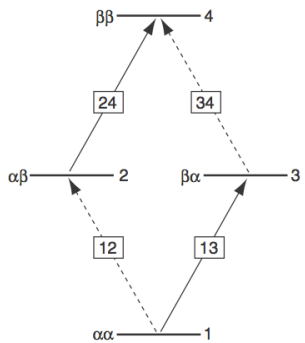

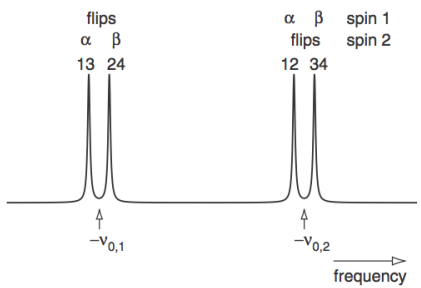

http://www-keeler.ch.cam.ac.uk/lectures/index.html

More complex cases of J-coupling

Additional splitting if coupled to multiple groups of (equivalent) protons

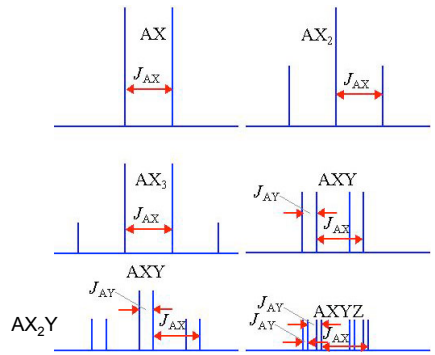

2nd order coupling in the AB case

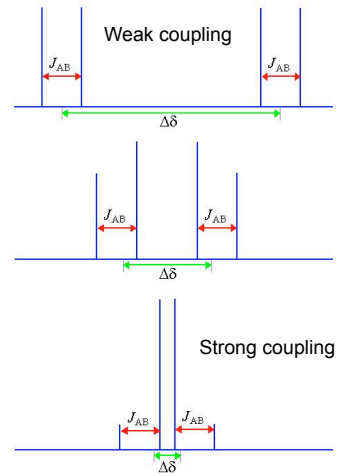

Sample NMR Spectra

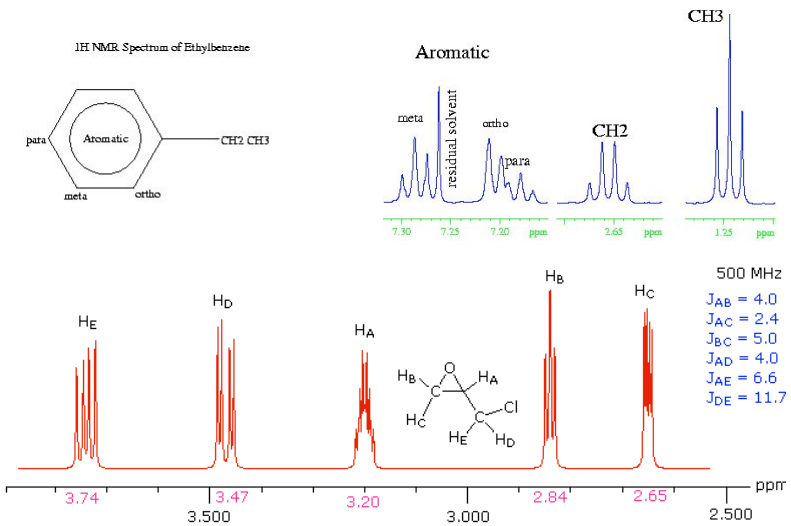

Typical J-Coupling Constants

Structural Type	J (Hz)
$H-C-(C)_n-C-H$	0 (unless in a rigid ideal orientation)
H_3C-CH_2-X	6 to 8
$(H_3C)_2CH-X$	5 to 7
$H-C(X)-C(Y)-H$	2 to 12 (depends on dihedral angle and the nature of X and Y)
$H-C-C(=O)-H$	0.5 to 3
H_2C	12 to 15 (must be diastereotopic)

Structural Type	J (Hz)
$H_2C=CH_2$	12 to 18
cis $H-C=C-H$	7 to 12
trans $H-C=C-H$	0.5 to 3
$H-C=C-C-H$	3 to 11 (depends on dihedral angle)
$H-C-C\equiv C-H$	2 to 3
benzene	o 6 to 9 m 1 to 3 p 0 to 1

http://www.cem.msu.edu/~reusch/VirtualText/Spectrpy/nmr/nmr1.htm

J-Coupling and Conformation

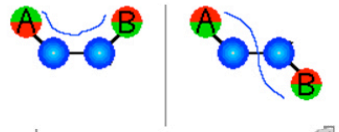

- J-coupling constants are very sensitive to conformations
  - A powerful mean to local structures
  - Minimal near 90 torsion and maximum near 0 or 180 torsion
- Karplus Equation: H-Y-Z-H
  - Empirical parameters (fitting)
  - Multiple solutions

$$J(\phi) = A\cos^2\phi + B\cos\phi + C$$

Y	Z	A	B	C
HC	CH	17	0	1.1
HC	NH	12	0	0.2
HC	OH	10	0	-1.0
HN	$C_\alpha H$ *	6.4	-1.4	1.9

(*: θ=Φ-60 for proteins)

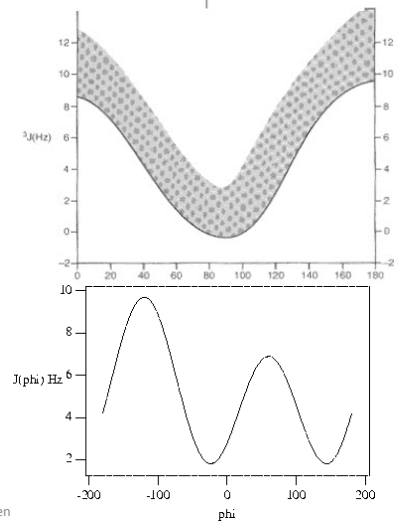

Relaxation

- Two types of relaxation processes
  - T_1: Spin-lattice relaxation (longitudinal relaxation, enthalpic relaxation): recovery of equilibrium populations (and thus a loss of signal and energy)
  - T_2: Spin-spin relaxation (transverse relaxation, entropic relaxation): lost of "coherence" (without a loss of excited state population or energy)
- T_2 is always smaller than T_1 (~ 0.1 – 20 sec).
- NMR peak width is generally determined by T_2.

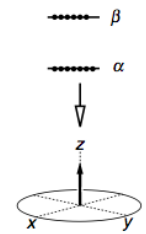

$$M_z(t) = M_{z,eq}\left(1 - e^{-t/T_1}\right)$$

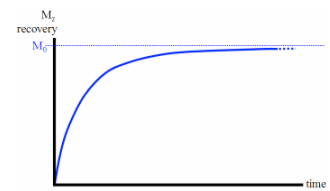

$$M_{xy}(t) = M_{xy}(0)e^{-t/T_2}$$

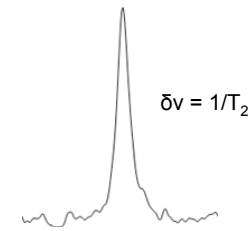

Molecular Tumbling and Relaxation

- Both processes are mainly related to molecular tumbling times (τ_c)
  - Tumbling time ~ ns (or w/ frequency of GHz)
  - Larger molecules tumbles slower and thus more effective in inducing relaxation (shorter T1, T2)
  - Faster relaxation at higher fields

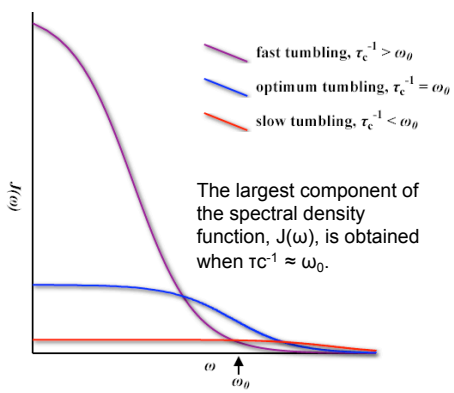

The largest component of the spectral density function, J(ω), is obtained when $\tau c^{-1} \approx \omega_0$.

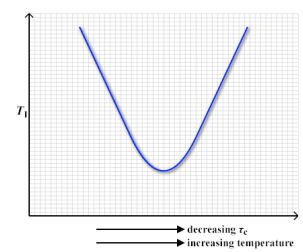

Nuclear Overhauser Effect (NOE)

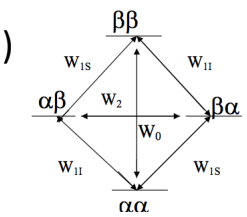

- RF saturation of one spin causes perturbation of spin population of nearby nuclei via magnetic dipole-dipole interactions. This changes the intensity of other spins.
- Difference spectrum with and without RF saturation of selected spin.
- Provide spatial distance info as dipolar coupling interacts throughout space.
- Generally an enhancement effect
- Magnitude further depends on molecular dynamics: slow motions (>ns) reduces NOE and might lead to negative NOE!
- NOE buildup rate~ $1/r^6$ (dipole-dipole)

$$\varepsilon_{NOE} = 1 + \frac{\gamma_I}{\gamma_S}\frac{(W_2 - W_0)}{W_0 + 2W_{1S} + W_2}$$

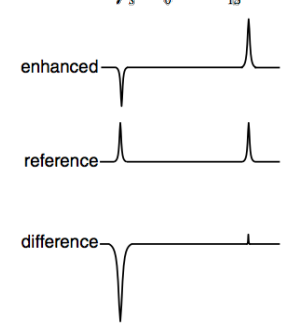

Summary of Information from NMR

- Chemical shifts: local chemical and structural environment
- (Integrated) intensity: number of protons/concentration
- J-coupling: adjacent protons and local conformations
- Relaxation times: dynamics (tumbling, internal and exchange)
- NOE: short-range spatial distance (< 6 Å) & (slow) dynamics

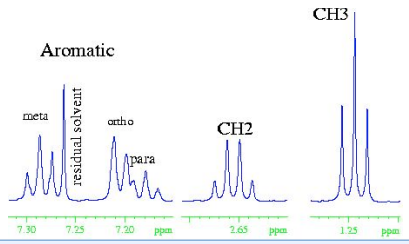

All these quantities can be accurately measured, often, for all nuclei in the system. This is why NMR can be extremely powerful.

Advanced Theories for Describing NMR

Development of modern 2D and multi-dimensional NMR techniques was made possible with the aid of special QM representation known as density-matrix formalism.

Additional reading: Dr. James Keeler's Lectures (U of Cambridge)
http://www-keeler.ch.cam.ac.uk/lectures/index.html

Vector Model

- Energy levels and selections severely limited in understanding advanced NMR techniques such as pulsed NMR and multidimensional NMR
- Vector model is the language of NMR: only rigorous in a few cases, but extremely useful even for the most sophisticated NMR experiments
- Bulk magnetization: net magnetization vector aligns with B_0

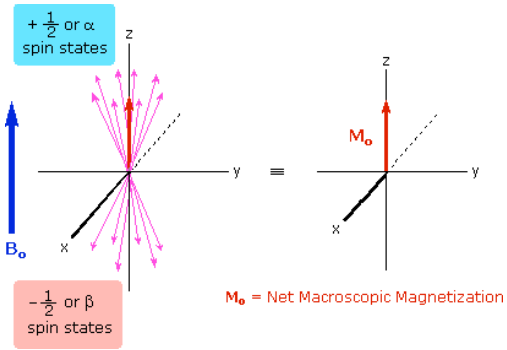

http://www.cem.msu.edu/~reusch/VirtualText/Spectrpy/nmr/nmr2.htm

Manipulation and Detection of M_o

- M_o might be "rotated" by a radiofrequency pulse.
- Once tilted away from the z axis, the magnetization vector rotates about the direction of the magnetic field sweeping out a cone with a constant angle at Larmor frequency (Larmor precession).
- NMR experiments detect the precession of the magnetization vector, such as by placing a small coil of wire round the sample, with the axis of the coil aligned in the *xy*-plane.
- Relaxations and free induction decay (FID)

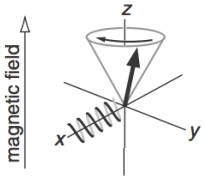

(only x coil shown)

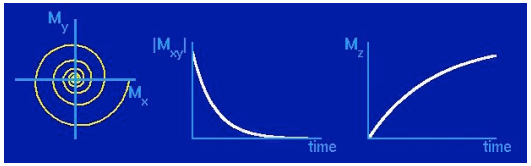

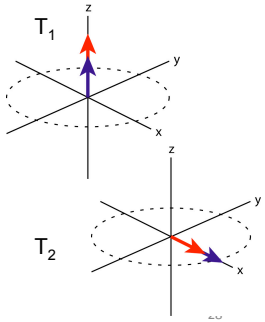

Spin Operators

- Bra-ket notation: $\int \psi_i^* \hat{Q} \psi_j d\tau \rightarrow \langle i|\hat{Q}|j \rangle$
  - spin states: $|\alpha\rangle$ and $|\beta\rangle$: $\langle\alpha|\alpha\rangle = 1$, $\langle\beta|\beta\rangle = 1$, and $\langle\alpha|\beta\rangle = 0$
- Spin angular momentum operators: I_x, I_y, and I_z (correspond to x, y, and z components of angular momemtum)
  - Spin stats $|\alpha\rangle$ and $|\beta\rangle$ are eigenstates of I_z: $I_z|\alpha\rangle = ½\,\hbar|\alpha\rangle$
  - I_x and I_y: $I_x|\alpha\rangle = \frac{1}{2}\hbar|\beta\rangle$ $\quad I_x|\beta\rangle = \frac{1}{2}\hbar|\alpha\rangle$ $\quad I_y|\alpha\rangle = \frac{1}{2}i\hbar|\beta\rangle$ $\quad I_y|\beta\rangle = -\frac{1}{2}i\hbar|\alpha\rangle$
- Hamiltonian: $H_{\text{free}} = \gamma B_0 \hbar I_z = \omega_0 I_z$ (single free spin)

  $H_{\text{free}} = \omega_{0,1} I_{1z} + \omega_{0,2} I_{2z} + 2\pi J_{12} I_{1z} I_{2z}$ (two weakly coupled spins)

number	spin states	energy
1	$\alpha\alpha$	$+\frac{1}{2}\nu_{0,1} + \frac{1}{2}\nu_{0,2} + \frac{1}{4}J_{12}$
2	$\alpha\beta$	$+\frac{1}{2}\nu_{0,1} - \frac{1}{2}\nu_{0,2} - \frac{1}{4}J_{12}$
3	$\beta\alpha$	$-\frac{1}{2}\nu_{0,1} + \frac{1}{2}\nu_{0,2} - \frac{1}{4}J_{12}$
4	$\beta\beta$	$-\frac{1}{2}\nu_{0,1} - \frac{1}{2}\nu_{0,2} + \frac{1}{4}J_{12}$

$$
\begin{aligned}
2\pi J_{12} I_{1z} I_{2z} |\beta_1\rangle|\alpha_2\rangle &= 2\pi J_{12} I_{1z}|\beta_1\rangle I_{2z}|\alpha_2\rangle \\
&= 2\pi J_{12} I_{1z}|\beta_1\rangle \tfrac{1}{2}|\alpha_2\rangle \\
&= 2\pi J_{12}\left(-\tfrac{1}{2}\right)|\beta_1\rangle \tfrac{1}{2}|\alpha_2\rangle \\
&= -\tfrac{1}{2}\pi J_{12}|\beta_1\rangle|\alpha_2\rangle
\end{aligned}
$$

Pulses

- The nuclear spin magnetization is manipulated by applying a magnetic field which is (a) transverse to the static magnetic field *i.e.* in the xy-plane, and (b) oscillating at close to the Larmor frequency of the spins.

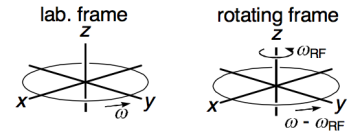

$$H = \omega_0 I_z + \omega_1 \cos(\omega_{\text{RF}} t) I_x \quad \text{(lab frame)}$$

$$H = (\omega_0 - \omega_{\text{RF}}) I_z + \omega_1 I_x \sim \omega_1 I_x \quad \text{(rotating f.)}$$

$$= \omega_1 I_{1x} + \omega_1 I_{2x} + \ldots \quad \text{(multiple spins)}$$

- What does a pulse do: change the direction of magnetization vector

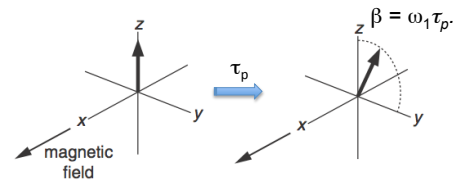

90 pulse: $\beta = 90^o$
180 pulse: $\beta = 180^o$
(x-pulse, y-pulse)

Hard pulse: large ω_1 (high power, short duration, larger bandwidth)

Soft pulse: small ω_1

Density Matrix Theory: Product Operator

- Recast of Schrödinger's equation to consider ensemble averaging
- Operators as matrix (in the eigenvector basis)
- Density matrix: $\sigma(t) = \overline{|\psi(t)\rangle\langle\psi(t)|}$

$$Q = \begin{pmatrix} \langle\alpha|Q|\alpha\rangle & \langle\alpha|Q|\beta\rangle \\ \langle\beta|Q|\alpha\rangle & \langle\beta|Q|\beta\rangle \end{pmatrix}$$

$$
\begin{aligned}
\sigma_{\text{eq}} &= P_{\text{av}} E + \Delta I_z \\
&= P_{\text{av}} \begin{pmatrix} 1 & 0 \\ 0 & 1 \end{pmatrix} + \Delta \begin{pmatrix} \frac{1}{2} & 0 \\ 0 & -\frac{1}{2} \end{pmatrix}
\end{aligned}
$$

$$
\begin{aligned}
I_z &= \begin{pmatrix} \langle\alpha|I_z|\alpha\rangle & \langle\alpha|I_z|\beta\rangle \\ \langle\beta|I_z|\alpha\rangle & \langle\beta|I_z|\beta\rangle \end{pmatrix} \\
&= \begin{pmatrix} \langle\alpha|\tfrac{1}{2}|\alpha\rangle & \langle\alpha|-\tfrac{1}{2}|\beta\rangle \\ \langle\beta|\tfrac{1}{2}|\alpha\rangle & \langle\beta|-\tfrac{1}{2}|\beta\rangle \end{pmatrix} \\
&= \begin{pmatrix} \frac{1}{2} & 0 \\ 0 & -\frac{1}{2} \end{pmatrix}
\end{aligned}
$$

- Observables as trace of matrix:

$$\overline{\langle Q \rangle} = \mathrm{Tr}[\sigma Q]$$

- Evolution of density matrix

$$\sigma(t) = \exp(-iHt)\sigma(0)\exp(iHt)$$

$$I_x = \begin{pmatrix} 0 & \frac{1}{2} \\ \frac{1}{2} & 0 \end{pmatrix} \qquad I_y = \begin{pmatrix} 0 & -\frac{i}{2} \\ \frac{i}{2} & 0 \end{pmatrix}$$

Additional reading: Dr. James Keeler's Lectures (U of Cambridge)
http://www-keeler.ch.cam.ac.uk/lectures/index.html

NMR Practice

NMR is becoming a "standard" tool. The key is now more to understand what it is capable and less about how one would actually carry out the (data acquisition) experiment.

Modern NMR Spectrometer

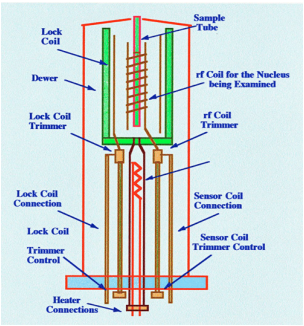

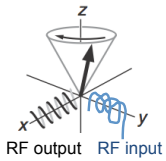

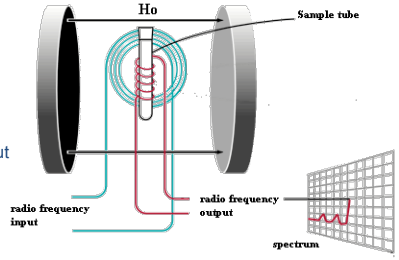

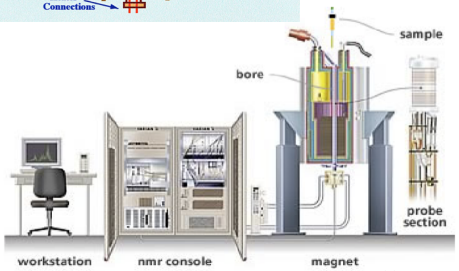

Fourier Transform NMR (FT-NMR)

- The basic pulse and acquire experiment

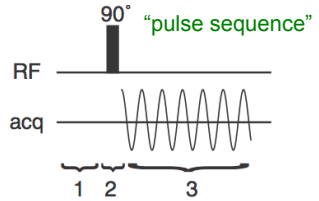

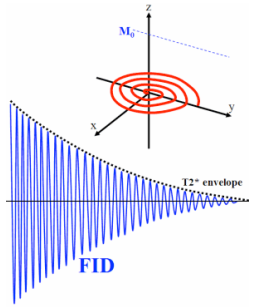

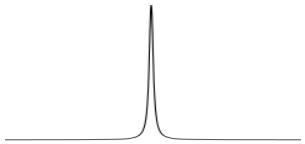

1. The sample is allowed to come to equilibrium.
2. RF power is switched on for long enough to rotate the magnetization through 90◦ i.e. a 90◦ pulse is applied. If the pulse is broad ("powerful") enough, all protons in the sample are exited.
3. After the RF power is switched off we start to detect the signal which arises from the magnetization as it rotates in the transverse plane.
4. The free induction decay contains information about oscillation of all protons. Fourier transform analysis will thus produce the whole NMR spectrum.

Magnetic moments of excess nuclear spins in the ground state are represented by vectors. The vectors precess about the direction of the B_o field.

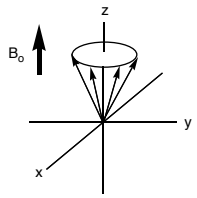

The sum of the individual spinvectors is represented by a large vector in the direction of the B_o field.

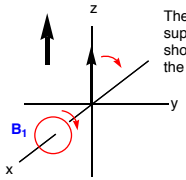

The B_1 field is supplied as a short pulse along the x-axis.

This causes the net magnetization to tip off the z-axis into the yz-plane and then precess about the z-axis. This is equivalent to ground spin states by absorption of energy from the B_1 field.

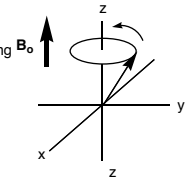

The net magnetization can be resolved into y- and z-axis components. The component in the xy-plane precesses about the z-axis.

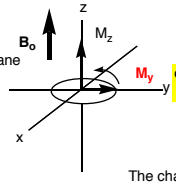

eye

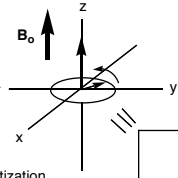

relaxation

The change in magnetization as a function of time as the net magnetization vector in the xy-plane precesses about the z-axis is observed along the y-axis as M_y.

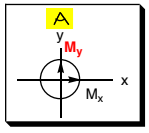

magnetization in the xy plane resolved into M_x and M_y components

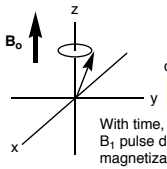

detector

With time, the change in net magnetization caused by the B_1 pulse decays back to the original state with no net magnetization in the xy-plane.

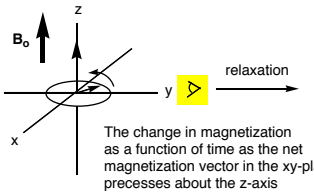

relaxation

The change in magnetization as a function of time as the net magnetization vector in the xy-plane precesses about the z-axis is observed along the y-axis as M_y.

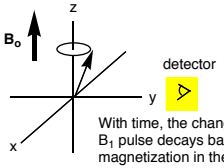

detector

With time, the change in net magnetization caused by the B_1 pulse decays back to the original state with no net magnetization in the xy-plane.

Magnetization along the y-axis as a function of time after the B_1 pulse.

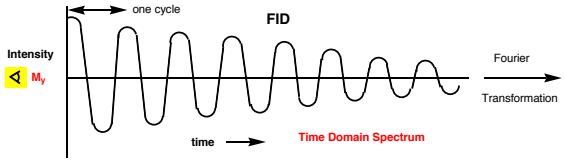

NMR Spectrum

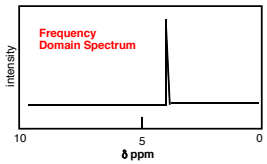

http://orgchem.colorado.edu/hndbksupport/nmrtheory/chemshift.html

NMR T_1 Relaxation

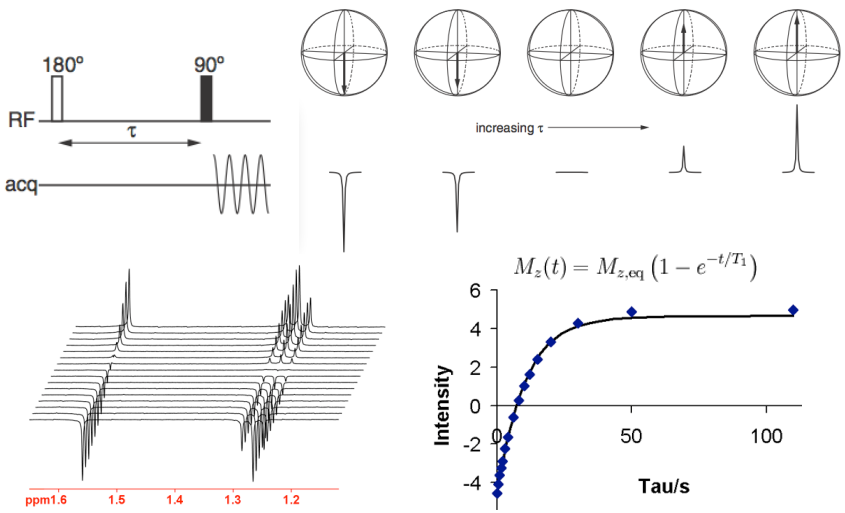

Spin Echo

The most famous NMR experiment: the magnetization ends up along the *same axis, regardless of the values of τ and the offset, Ω*. This is achieved by using 180 pulse as refocusing pulse.

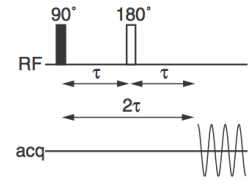

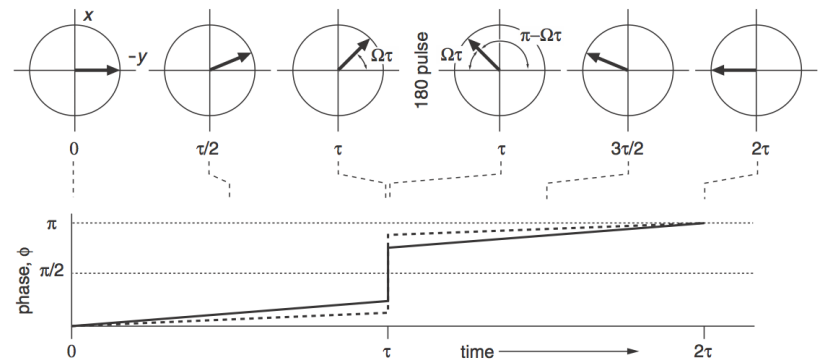

Coherence

- At equilibrium, (phase) of transverse magnetization is completely random and averages to zero, i.e., no coherence.
- Upon applying a RF pulse (say, a 90 pulse along -x), the net magnetization along z-axis is now "rotated" to align along y-axis. This excitation: 1) remove the population difference of two spin states (no net magnetization along z), and 2) establishes a "coherence": the nuclei now process with the same phase (on an average sense).
- Through collision, the coherence is gradually lost (before the equilibrium population is fully re-established)

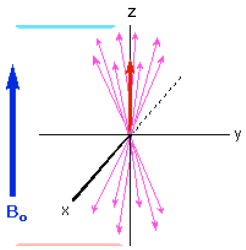

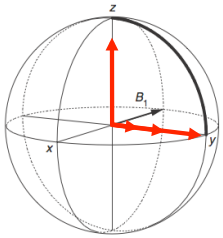

90 pulse along -x

T_2 Relaxation Measurement

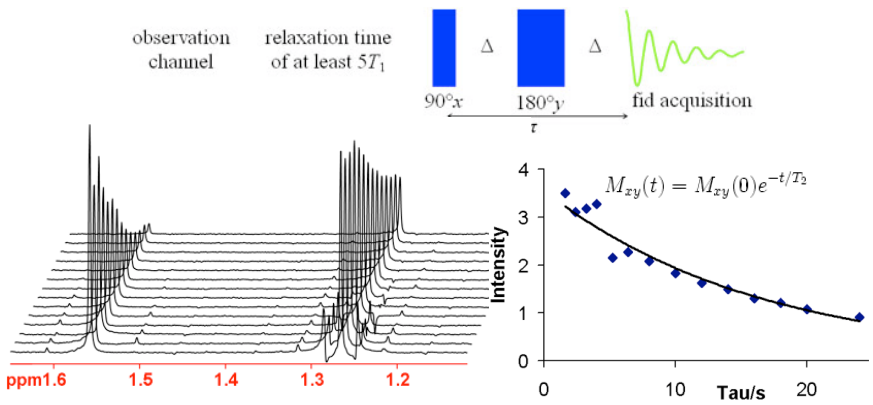

http://chem.ch.huji.ac.il/nmr/techniques/other/t1t2/t1t2.html

Phase Cycling

- To eliminate unwanted signals/artifacts (and select desired coherence)
- By repeating the (1D) experiment with alternating pulse phases and averaging the FIDs, certain signals (and artifacts) will cancel. Another direct benefit is enhancement of selected signal-to-noise ratio.
- Example: **PAPS** (Phase Alternating Pulse Sequence)

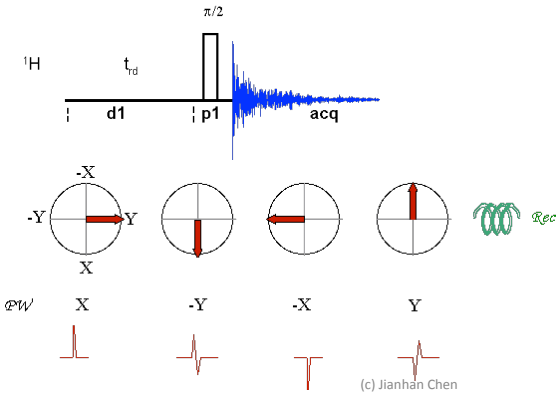

Scan	Pulse	Receiver
1	X	X
2	-Y	-Y
3	-X	-X
4	Y	Y

These signals add up to zero! (unless receiver phase follows pulse

Artifacts that do not follow the phases will cancel out!

1D NMR of Proteins

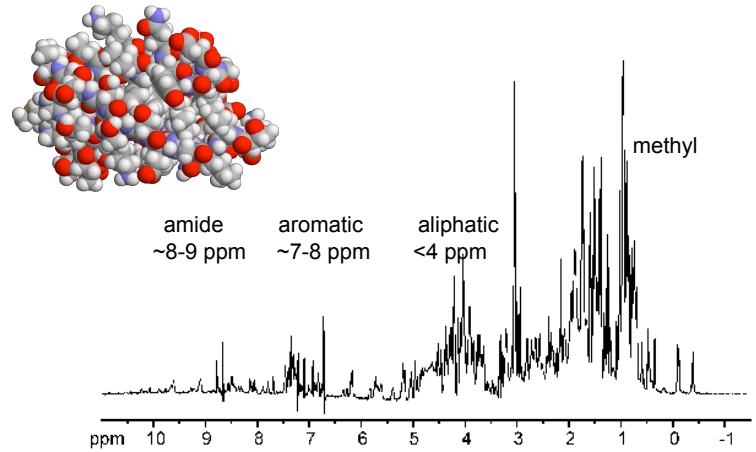

Multi-dimensional NMR is the work-horse in biomolecular studies.

2D NMR Spectroscopy

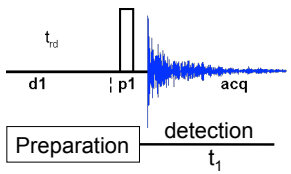

FID: $C(t_1)$ $\xrightarrow{FT}$ Spectrum $I(\upsilon_1)$

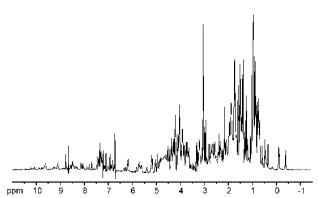

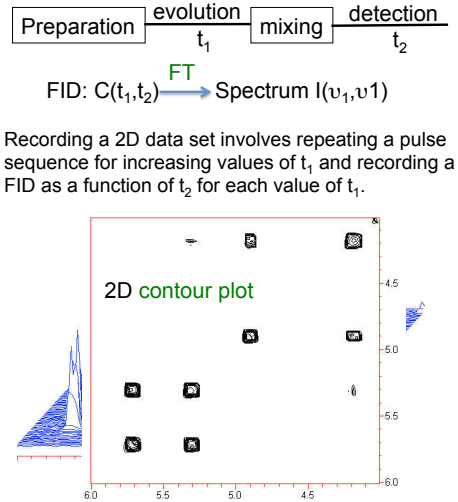

FID: $C(t_1,t_2)$ $\xrightarrow{FT}$ Spectrum $I(\upsilon_1,\upsilon 1)$

Recording a 2D data set involves repeating a pulse sequence for increasing values of t_1 and recording a FID as a function of t_2 for each value of t_1.

Correlation Spectroscopy (COSY)

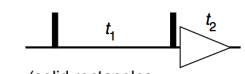

(solid rectangles denote 90 pulses)

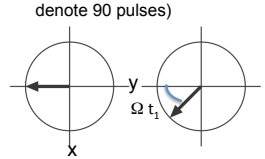

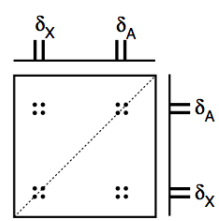

Schematic COSY spectrum for two coupled spins, A and X

First 90 pulse: $I_{1z} \xrightarrow{\pi/2 I_{1x}} \xrightarrow{\pi/2 I_{2x}} -I_{1y}$

This state then evolves for time t_1, first under the influence of the offset of spin 1 (that of spin 2 has no effect on spin 1 operators):

$$-I_{1y} \xrightarrow{\Omega_1 t_1 I_{1z}} -\cos\Omega_1 t_1\, I_{1y} + \sin\Omega_1 t_1\, I_{1x}$$

Both terms on the right then evolve under the coupling

$$-\cos\Omega_1 t_1\, I_{1y} \xrightarrow{2\pi J_{12} t_1 I_{1z} I_{2z}} -\cos\pi J_{12} t_1 \cos\Omega_1 t_1\, I_{1y} + \sin\pi J_{12} t_1 \cos\Omega_1 t_1\, 2I_{1x} I_{2z}$$

$$\sin\Omega_1 t_1\, I_{1x} \xrightarrow{2\pi J_{12} t_1 I_{1z} I_{2z}} \cos\pi J_{12} t_1 \sin\Omega_1 t_1\, I_{1x} + \sin\pi J_{12} t_1 \sin\Omega_1 t_1\, 2I_{1y} I_{2z}$$

(For AX system: $H_{\text{free}} = \omega_{0,1} I_{1z} + \omega_{0,2} I_{2z} + 2\pi J_{12} I_{1z} I_{2z}$)

Second 90 pulse:

$$-\cos\pi J_{12} t_1 \cos\Omega_1 t_1\, I_{1y} \xrightarrow{\pi/2 I_{1x}} \xrightarrow{\pi/2 I_{2x}} -\cos\pi J_{12} t_1 \cos\Omega_1 t_1\, I_{1z} \qquad \{1\}$$

$$\sin\pi J_{12} t_1 \cos\Omega_1 t_1\, 2I_{1x} I_{2z} \xrightarrow{\pi/2 I_{1x}} \xrightarrow{\pi/2 I_{2x}} -\sin\pi J_{12} t_1 \cos\Omega_1 t_1\, 2I_{1x} I_{2y} \qquad \{2\}$$

$$\cos\pi J_{12} t_1 \sin\Omega_1 t_1\, I_{1x} \xrightarrow{\pi/2 I_{1x}} \xrightarrow{\pi/2 I_{2x}} \cos\pi J_{12} t_1 \sin\Omega_1 t_1\, I_{1x} \qquad \{3\}$$

$$\sin\pi J_{12} t_1 \sin\Omega_1 t_1\, 2I_{1y} I_{2z} \xrightarrow{\pi/2 I_{1x}} \xrightarrow{\pi/2 I_{2x}} -\sin\pi J_{12} t_1 \sin\Omega_1 t_1\, 2I_{1z} I_{2y} \qquad \{4\}$$

Only last (3) and (4) terms lead to observable signals. Term 3 yields diagonal peaks (Ω_1, Ω_1). Term 4 contains "coherence transfer": a (Ω_1, Ω_2) cross-peak modulated by Ω_1 in t_1 and by Ω_1 in t_2.

Information from COSY

- Most rigorous way of assigning protons: presence of cross-peaks unambiguously reveal J-coupling connectivity
- Patterns of connectivity is characteristic of the molecule: once a single peak (e.g., methyl) is assigned, the rest follow the COSY connectivity.
- J-coupling constants also measured.

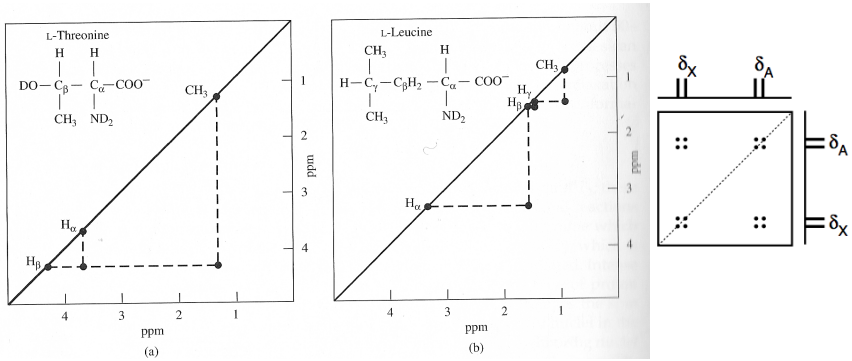

NOESY/EXSY

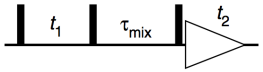

after t_1: $-I_{1y} \xrightarrow{\Omega_1 t_1 I_{1z}} -\cos\Omega_1 t_1\, I_{1y} + \sin\Omega_1 t_1\, I_{1x}$

2nd 90 pulse: $-\cos\Omega_1 t_1\, I_{1y} \xrightarrow{\pi/2 I_{1x}} \xrightarrow{\pi/2 I_{2x}} -\cos\Omega_1 t_1\, I_{1z}$ 1)

$\sin\Omega_1 t_1\, I_{1x} \xrightarrow{\pi/2 I_{1x}} \xrightarrow{\pi/2 I_{2x}} \sin\Omega_1 t_1\, I_{1x}$ 2)

First term is "frequency labeled" and undergo NOE/chemical exchange; second term is eliminate by coherence selection (via phase cycling). The 3rd pulse detects the first term.

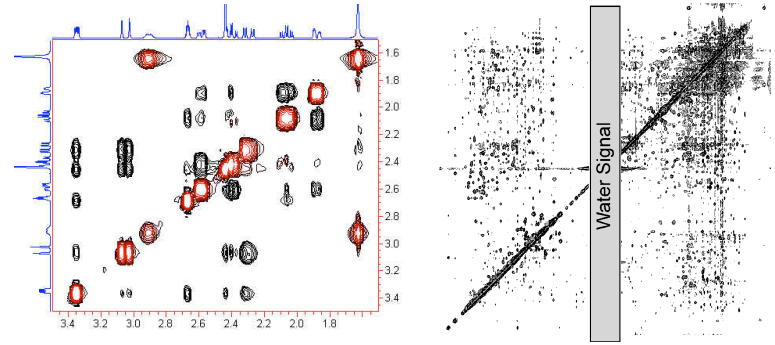

Coherence Selection

- Phase cycling and gradient pulses to select/eliminate certain types of coherence excitation for detection

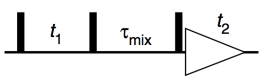

NOESY/EXSY

after t_1: $-I_{1y} \xrightarrow{\Omega_1 t_1 I_{1z}} -\cos\Omega_1 t_1\, I_{1y} + \sin\Omega_1 t_1\, I_{1x}$

2nd 90 pulse: $-\cos\Omega_1 t_1\, I_{1y} \xrightarrow{\pi/2 I_{1x}} \xrightarrow{\pi/2 I_{2x}} -\cos\Omega_1 t_1\, I_{1z}$ 1)

$\sin\Omega_1 t_1\, I_{1x} \xrightarrow{\pi/2 I_{1x}} \xrightarrow{\pi/2 I_{2x}} \sin\Omega_1 t_1\, I_{1x}$ 2)

How do one "select" I_{1z} for detection?

A simplified scheme (the actual phase cycling is more complicated):

Scan 1: apply 2nd 90 pulse along x
Scan 2: apply 2nd 90 pulse along –x

At the end, subtract FIDs from two scans. Can you imagine what happens to the above two terms?

Heteronuclear Single Quantum Correlation (HSQC)

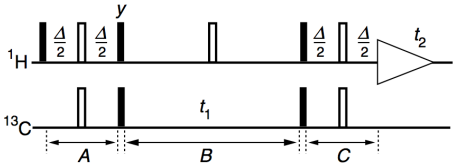

Filled rectangles represent 90° pulses and open rectangles represent 180° pulses. The delay $\Delta = 1/(2J_{12})$; all pulses have phase x unless otherwise indicated.

- Most frequently recorded in protein NMR
- Utilize one-bond C/N-H coupling
- Excitation and detection in proton channel for best sensitivity! (why?)
- One cross-peak (group) for each C/N-H pair
- Key information obtained: chemical shifts!
- Quick and simple: rapid NMR feasibility diagnosis and stability monitoring of protein samples

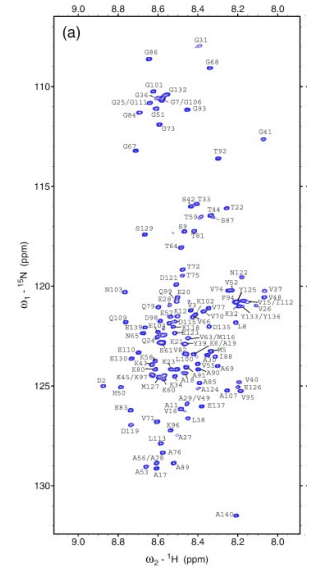

Multi-Dimensional NMR

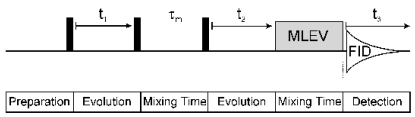

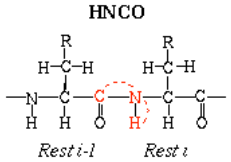

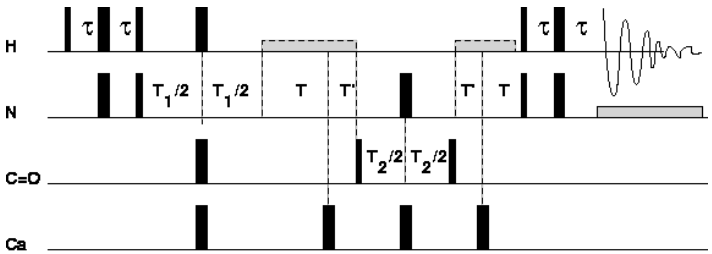

HNCO (circa 1990)

3D Spectra

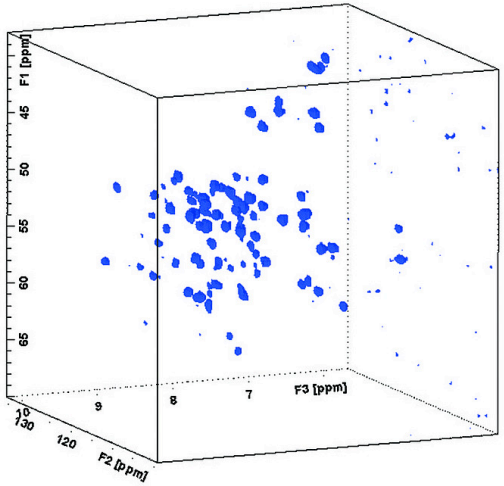

Visualizing 3D Spectra using Strips

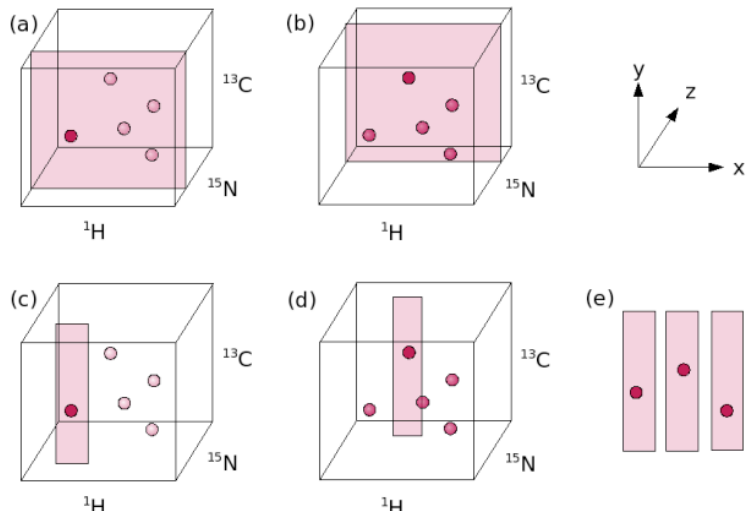

http://www.protein-nmr.org.uk/assignment_theory.html

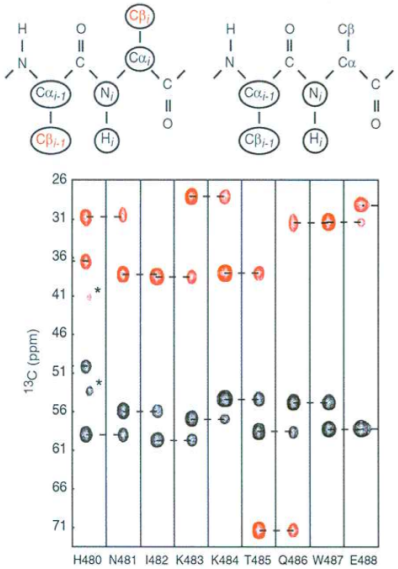

… Schematic representations of dipeptides showing nuclei in residues i and i¡1, where i is the residue number, that are correlated (circled) in the HNCACB (top left) and (HB) CBCA(CO)NNH experiments (top right). The 13CB nuclei observed in the HNCACB are colored red, denoting the opposite phase of signals arising from these spins relative to phases of 13CA signals. Strip plots from the HNCACB experiment are at the 1HN(i) and 15N(i) chemical shifts for residues His 480 to Glu 488 of the Nedd4 WW domain (bottom). The negative 13CB signals are represented as red contours. Correlations between sequential 13CA/13CB resonances are indicated by dotted lines. The asterisks (¤) in the His 480 strip identify peaks with increased intensity on another plane. This spectrum was recorded at 500 MHz (1H frequency) on a 1-mM 15N=13C-labeled Nedd4 WW domain bound to the unlabeled ENaCBP2 peptide in 10 mM sodium phosphate, 90% H2O, 10% D2O, pH 6.5 at 30±C …

Multidimensional NMR Methods for Protein Structure Determination, Kay et al., IUBMB Life (2001).

Triple Resonance Protein NMR

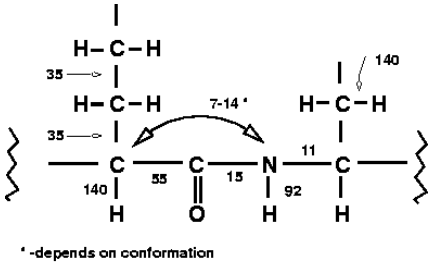

Scalar Couplings in Proteins

Labeling of a protein with both ^{15}N & ^{13}C causes almost all of the atoms in the protein to become observable in NMR spectroscopy. More importantly, all of the atoms also become scalar coupled to each other. These homonuclear and heteronuclear scalar couplings are relatively large compared to the linewidth of the resonance lines.

Two key references:

1. Markley (1994) Methods in Enzymology Vol 239.
2. Bax & Grzesiek (1993), Accounts of Chemical Research, 26, 132.

Multidimensional Protein NMR

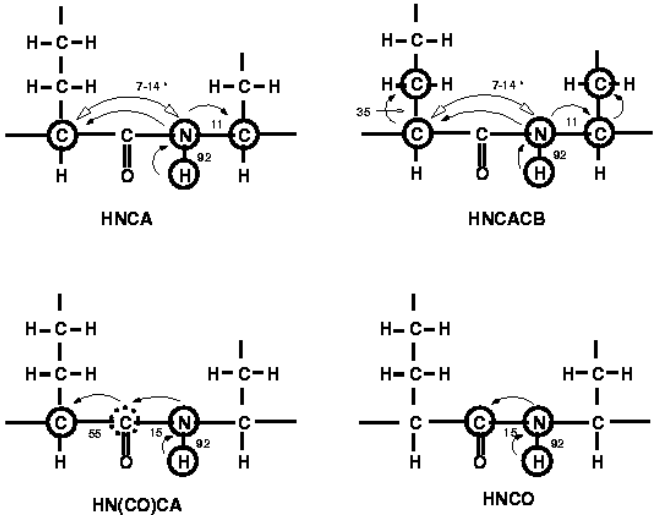

Multidimensional Protein NMR

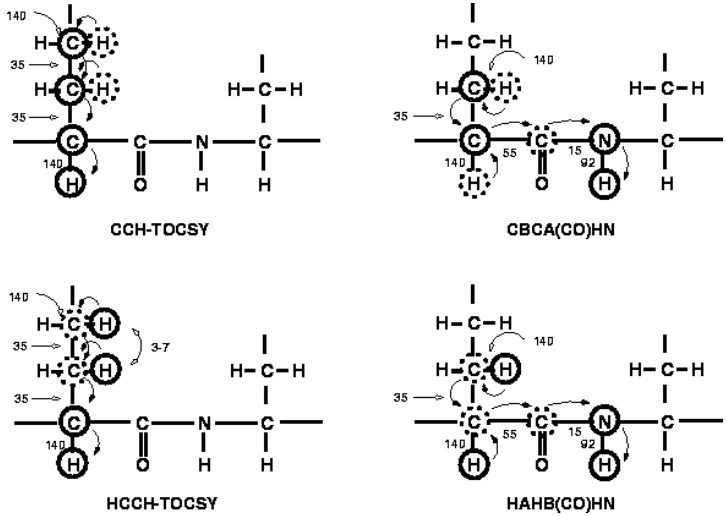

Biomolecular NMR Applications

1. High-resolution structure determination
2. Dynamics: relaxation analysis
3. Transient interactions: excitation transfer, spin-labeling
4. Solid state: membrane proteins
5. In-cell NMR
6. Imaging: MRI

....

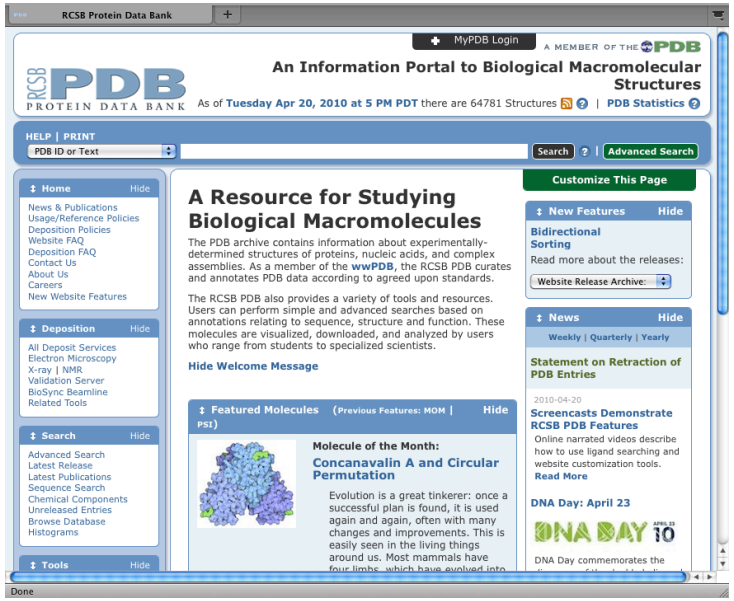

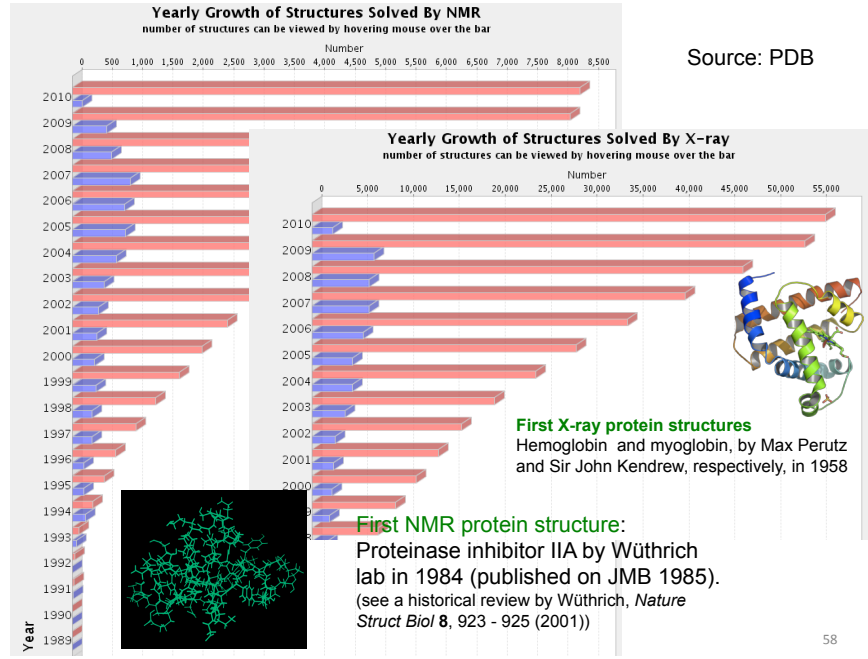

Source: PDB

1. High-resolution NMR structure determination

- NMR is one of the only two methods for high-resolution structure determination besides X-ray crystallography
- Advantages of NMR
  - In solution: more physiologically relevant conditions
  - Provide information on protein dynamics
  - Room temperature or (almost) any temperatures of interest
  - Direct monitoring of biophysical and biochemical processes
- Limitations of NMR
  - Time consuming and labor intensive: difficult for high-throughput, prone to human errors, less precise
  - Need to be highly soluble: stable with near mM concentration
    - Sometimes "strange" NMR buffers have to be used
  - Limited to protein of moderate sizes: < 200 residues in general
- X-ray and NMR can be complementary

Basic Steps of NMR Structure Determination

- Sample preparation and data collection
- Chemical shift assignments: backbone and sidechain
  - Chemical Shift Indexing and J-coupling constants: 2nd structures
- Distance and other structural restraints: NOESY
- Structural calculations: restrained molecular dynamics
- Refinement and validation

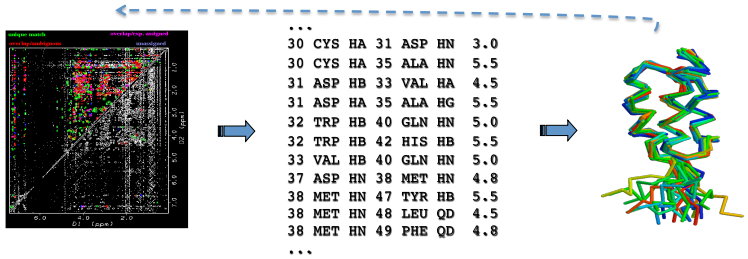

Also see: http://en.wikipedia.org/wiki/Protein_nuclear_magnetic_resonance_spectroscopy

Protein NMR Sample Requirements

- Efficient preparation of sufficient highly purified material with appropriate isotope labeling is increasingly the rate limiting step in NMR studies of biomacromolecules
  - typically expressing proteins in minimal medium with single C13 and N15 resources (glucose and ammonium salt)
- All typical NMR sample requirements apply: D2O, no paramagnetic ions, clean tube, degassing, reference, etc
- Buffer: pH, ions, and co-solvent: tricky, optimized (solubility, stability, structural properties, etc)
- Quick view of NMR suitability: HSQC (H/C or H/N)

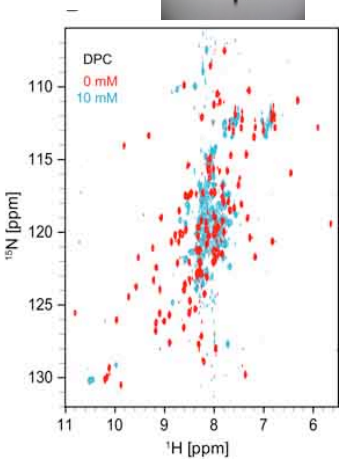

Small Peptides (<30 residues)

- 2D Proton NMR only: isotope enrichment not necessary!
- Backbone and sidechains assigned using COSY and TOCSY
- Proton-proton distance from NOESY

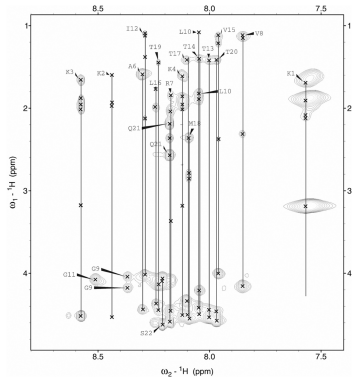

Finger print region (HN-Ha/Side chain protons) of 1H-1H TOCSY

p22 in SDS micelles
KKKKP ARVGL GITTV LTMTT QS

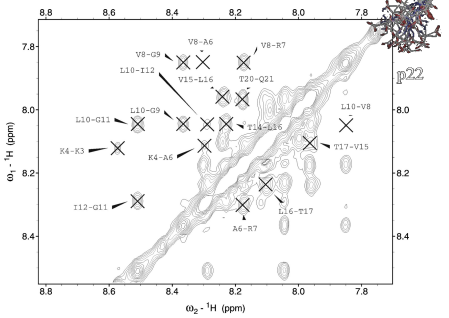

Finger print region (H^N-H^N) of 2D ^{1}H-^{1}H NOESY spectrum

Herrera et al PROTEINS (in press)

TOCSY

Creates correlations between all protons within a given spin system, not just between close neighbors like in COSY. Particularly useful in identification of amino acids!

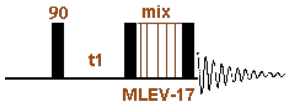

"spin lock period"

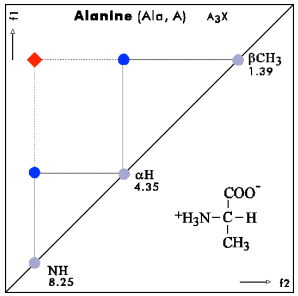

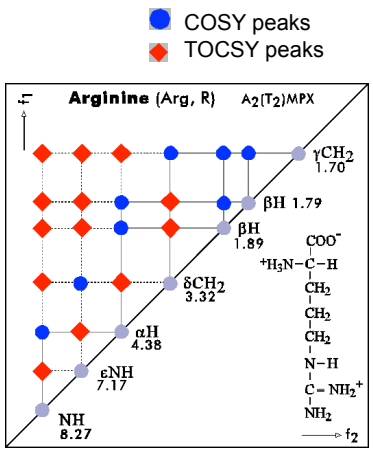

Spin Lock

Spin-echo sequence

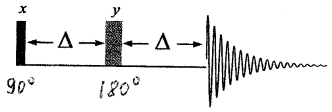

Spin-lock sequence

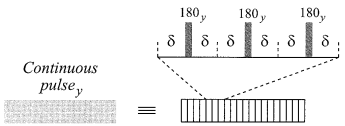

Spin-lock sequence – is the Spin-echo sequence, applied continuously. The simplest spin-lock sequence is just a continuous pulse.

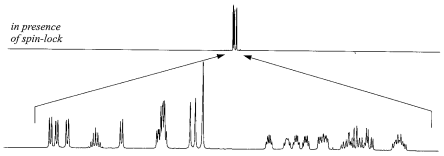

The Spin-lock sequence makes all spins strongly coupled (differences in chemical shifts are less than coupling constants)

Larger Proteins

- CS assignment requires doubly-labeled proteins
- Automatic assignment often feasible: correct assignment a critical starting point!

High resolution ^{1}H-^{15}N HSQC
High resolution ^{1}H-^{13}C HSQC (aliphatic)
High resolution ^{1}H-^{13}C HSQC (aromatic)

Backbone: HNCA
HN(CO)CA
HNCO
HCACO
HN(CA)CO
CBCA(CO)NH
HNCACB
HBHA(CBCACO)NH
HN(CA)HA

Side chain: ^{15}N TOCSY-HSQC
C(CO)NH-TOCSY
H(CCO)NH-TOCSY
CCH-TOCSY
CCH-COSY
HCCH-TOCSY
HCCH-COSY
Aromatic
^{1}H spectra (2QF COSY and 2Q) for resonances within aromatic rings
^{1}H NOESY to connect Hd with Hb (marked high intensity NOEs)
(Hb)Cb(CgCd)Hd
(Hb)Cb(CgCdCe)He
(HC)C(C)CH-TOCSY
Methionine
HMBC to assign methyl group

Incomplete excerption from Wright/Dyson lab manual (The Scripps Research Institute).

Distance Restraints from NOE

- Data Acquisition:

  3D ^{15}N NOESY
  3D ^{13}C NOESY
  4D ^{15}N, ^{13}C NOESY
  4D ^{13}C, ^{13}C NOESY
  3D ^{15}N, ^{15}N NOESY
  3D ^{15}N HSQC-NOESY-HSQC
  (take two NOESY spectra at 2 or more mixing times when possible)

- Calibration of NOE
  - NOE buildup ~ $1/r^6$
  - Actual slope also depends on dynamics, spin diffusion, strong coupling etc
  - NOESY is noisy!
  - Utilize known distances: intra-residue ones, 2nd structures

- NOE assignments: overlaps lead to ambiguous NOEs; iterative assignment assisted with structural feedbacks!
- Binning NOE intensities: large uncertainties and only qualitative!

class	restraint	description *for protein w/ M_r<20 kDa
strong	1.8-2.7 Å	strong intensity in short t_m (~50 ms*) NOESY
medium	1.8-3.3 Å	weak intensity in short t_m (~50 ms*) NOESY
weak	1.8-5.0 Å	only visible in longer mixing time NOESY

3D NOESY-HSQC

- 2D ^{1}H-^{1}H NOESY can be very crowded.
- Additional dimension helps to disperse the peaks and facilitate assignment
- NOESY followed by HSQC

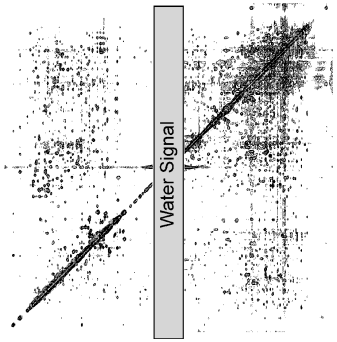

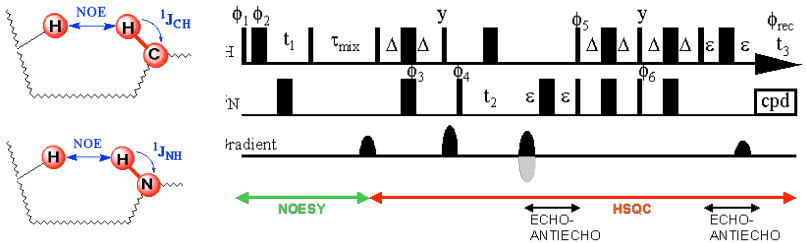

3D 1H-15N NOESY-HSQC spectrum of a dimeric GpA mutant

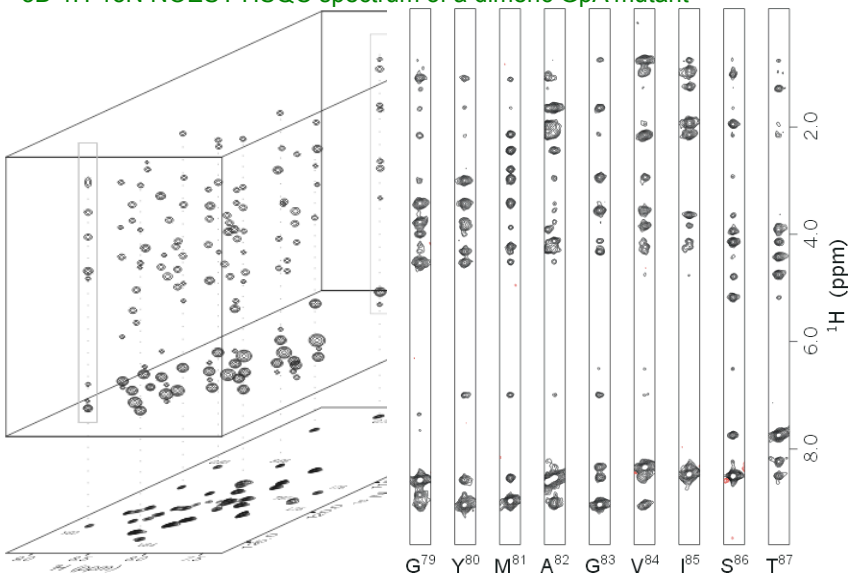

http://www-bioc.rice.edu/~mev/spectra3.html

Additional Structural Restraints

- Chemical shift analysis: CSI
- Hydrogen bonds: D_2O exchange experiments to identify slow exchanging amides (those involved in h-bonds)
- J-coupling constants

Experiment	Coupling constant	Information
HNHA	$^3J_{HN,Ha}$	ϕ
HA(CA)HB COSY	$^3J_{Ha,Hb}$	c_1, bH stereos
HNHB	$^3J_{HN,Hb}$	c_1, bH stereos
2QF COSY	$J_{HN,Ha}$, $^3J_{Ha,Hb}$	confirmation
^{13}C-{^{13}CO} spin-echo difference ct-HSQC	$^3J_{Cg,CO}$	Ile, Thr χ_1, Val χ_1, $C\gamma$ stereos
^{13}C-{^{15}N} spin-echo difference ct-HSQC	$^3J_{Cg,N}$	Ile, Thr χ_1, Val χ_1, $C\gamma$ stereos

Structural Calculation

- All structural restraints implemented by penalty functions

$$V = \sum V_{MM} + \sum V_{NMR}$$

$$V_{NOE}(ij) = 0, \quad \text{for} \quad r_{ij,low} \le r_{ij} \le r_{ij,up} \qquad (2.24a)$$

$$V_{NOE}(ij) = k_{NOE}(r_{ij} - r_{ij,low})^2, \quad \text{for} \quad r_{ij,low} \ge r_{ij} \qquad (2.24b)$$

$$V_{NOE}(ij) = k_{NOE}(r_{ij} - r_{ij,up})^2, \quad \text{for} \quad r_{ij,up} \le r_{ij} \qquad (2.24c)$$

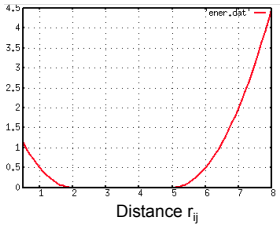

- Structural calculation re-casted as global energy minimization/ conformational search problem (which is molecular dynamics all about!)
- Restrained molecular dynamics with simulated annealing to generate sets of structures that maximally satisfy all restraints
- Two key popular NMR structural calculation software
  - CYANA/DYANA: http://www.las.jp/prod/cyana/eg
  - CNS: http://cns-online.org/v1.21/
  - Xplor-NIH: http://nmr.cit.nih.gov/xplor-nih/

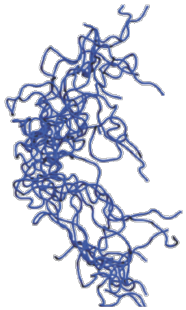

Overview of Structure Calculations

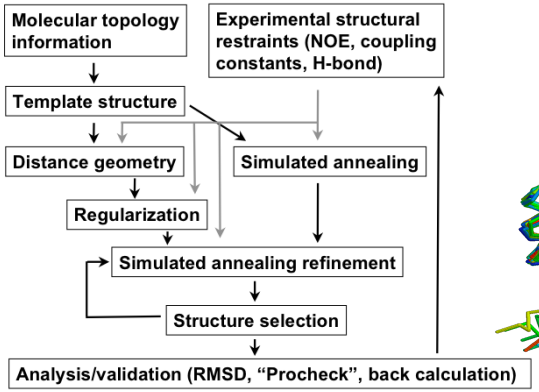

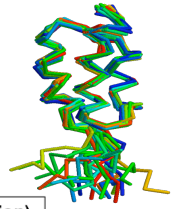

Adapted from Brünger, A. T., "X-PLOR Version 3.1, A System For X-ray Crystallography and NMR"

Simulated Annealing

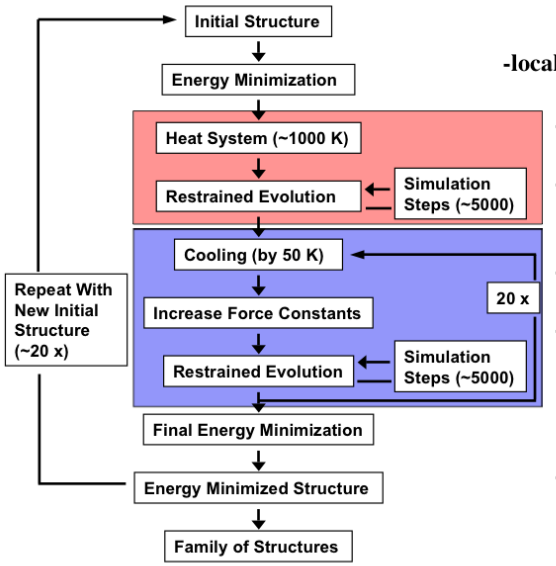

-local energy minimum reached

-heat system to cross local energy barriers
-atomic positions determined from velocities/accelerations

-slow reduction of atomic velocities (many steps)
-increase weights of experimental restraints

-global energy minimum?

Internal Coordinate MD

Based on figure from Horst Joachim Schirra Max-Planck Institute for Biochemistry
http://www.cryst.bbk.ac.uk/pps2/projects/schirra/html/home.htm

Refinement & Validation

- NMR restraint violation statistics: self-consistency
- Convergence (precision): can be misleading
- PROCHECK: PDB statistics on general ϕ/ψ distributions
- Refinement using additional information from
  - Empirical protein force field: solvent effects

$$V = \sum V_{MM} + \sum V_{NMR} + \sum V_{Other}$$

  - Additional experimental data: NMR and non-NMR!
  - Residual dipolar coupling (RDC)

Table 1. Structural statistics for the RPP29–RPP21 complex

	RPP29	RPP21
NMR constrains		
NOEs	2038	1407
Intraresidue ($i-j=0$)	833	606
Sequential ($i-j=1$)	475	364
Short range ($1<i-j<5$)	204	203
Long range ($i-j>5$)	526	234
Intermolecular (RPP29 – RPP21)	472	
Ambiguous	376	328
Hydrogen bonds[a]	38	80
Dihedral angles	188	162
Structure statistics		
Violations		
Distance violations >0.5 Å	1.50±1.02	
Dihedral angle violations >5°	1.63±0.10	
Deviation from idealized geometry		
Bonds (Å)	0.0046±0.00008	
Angles (°)	0.77±0.02	
Impropers (°)	0.56±0.01	
Ramachandran statistics (%)[b]		
Favored	77.0	
Additionally allowed	21.1	
Generously allowed	1.4	
Disallowed	0.5	
Precision (RMSD form the mean structure)[c]		
Backbone atoms (Å)	0.58	
All heavy atoms (Å)	0.87	

PDB: 2KI7; Xu et al, JMB (2009)

Refinement in implicit solvent can be used to obtain native-like models from limited NMR data.

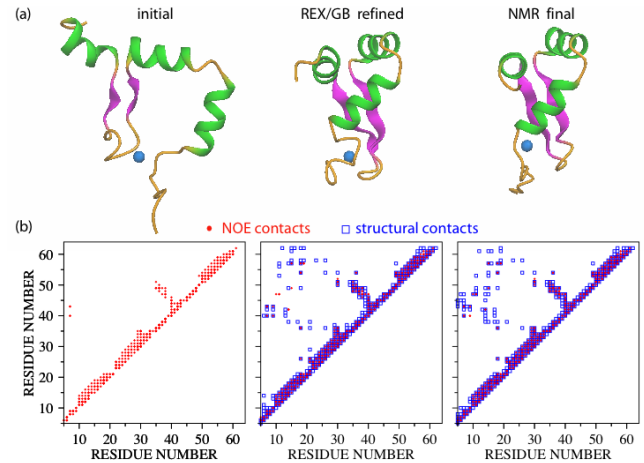

Cost: ~12h wall time using 16 Intel 2.4GHz CPUs

Chen et al., *J. Biomol NMR* (2004).

Refinement of Maltose-Binding Protein (MBP)

- 370 residues, 42 kDa
- 1943 NOE, 45 hydrogen bonding and 555 dihedral angle restraints.
- Average backbone RMSD to X-ray structure is 5.5 Å (a).
- Improved to 3.3 Å with 940 additional dipolar coupling based restraints (b).

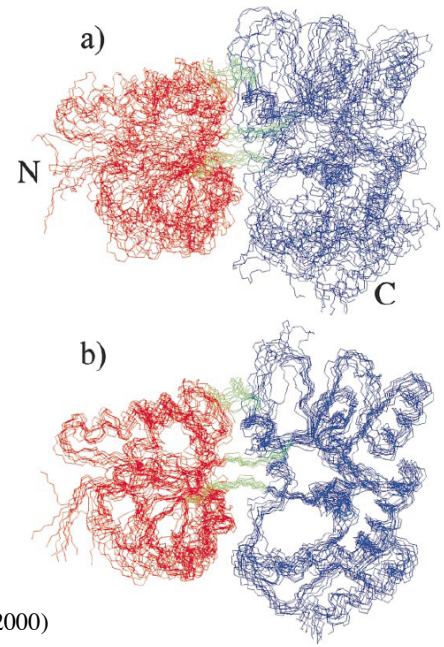

Ref. Mueller *et al*., JMB **300**, 197 (2000)

Implicit Solvent Refinement Results

- All NOE and dihedral angle restraints were used.
- 48 replicas were simulated at 300 to 800 K until converged.
- Total of 1.0 ns REX/GB simulation.

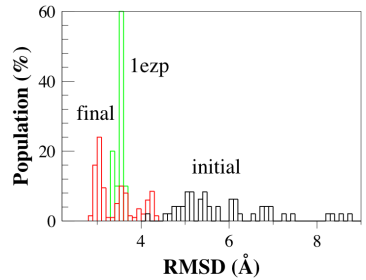

	Initial	Final
RMSD to X-ray (Å) [a]		
Global	4.3±4.1	2.3±2.6
N-domain	2.5±2.1	2.2±1.4
C-domain	3.0±3.2	2.0±1.9
ϕ/ψ space: residues (%)		
Most favored	72.2	84.3
Additionally allowed	22.8	13.3
Generously allowed	3.8 1.6	
Disallowed	1.2	0.8
Violation statistics		
RMSD of NOEs (Å)	0.0047	0.014
NOE violations (> 0.2Å)	2.85	4.42
RMSD of angles (in degrees)	0.53	6.25

[a] Backbone RMSD with respect to PDB:1dmb shown. Global: residues 6-235 and 241-370; N-domain: 6-109 and 264:309; C-domain: 114-235, 241-258 and 316-370.

Chen et al., *JACS* (2004).

Representative Structures: MBP

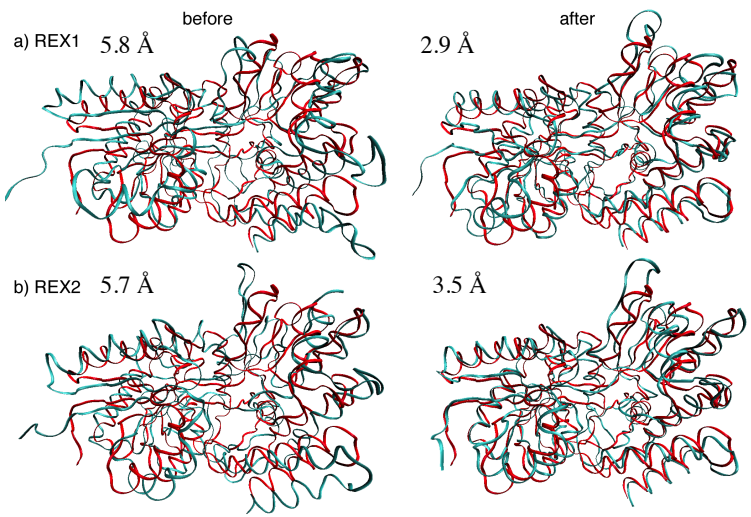

RMSD values: from X-ray (PDB:1dm); backbone atoms of residues 6-235 and 241-370

Automatic/High Throughput NMR Structure Determination

"The automation of protein structure determination using NMR is coming of age. The tedious processes of resonance assignment, followed by assignment of NOE (nuclear Overhauser enhancement) interactions (now intertwined with structure calculation), assembly of input files for structure calculation, intermediate analyses of incorrect assignments and bad input data, and finally structure validation are all being automated with sophisticated software tools. The robustness of the different approaches continues to deal with problems of completeness and uniqueness; nevertheless, the future is very bright for automation of NMR structure generation to approach the levels found in X-ray crystallography. Currently, near completely automated structure determination is possible for small proteins, and the prospect for medium-sized and large proteins is good."

Table 1

Summary of programs for automated structure calculation.

Program	References	MD engine	Utility
ARIA	[34,35,36*,37]	CNS XPLOR	Ambiguous NOE restraint generation, spin diffusion correction, iterative structure calculation, analysis
AutoStructure	[28,31*]	XPLOR CNS DYANA	NOE, torsion angle and hydrogen bond restraint generation, NOESY assignment, iterative structure calculation, analysis
BACUS/CLOUDS	[38**,39,40]		NOESY assignment, distance matrix calculation
CANDID/ATNOS	[41,42]	DYANA	NOESY peak analysis, NOESY peak assignment, restraint generation, iterative structure calculation
NOAH	[32,33]	DIAMOD DIANA	NOESY assignment, NOE restraint generation, torsion angle restraints, iterative structure calculation
SANE	[47]	AMBER DYANA	NOESY assignment, restraint generation, structure calculation
PASD	[43**]	XPLOR-NIH	Probability analysis of NOE restraints and simultaneous structure calculation

MD, molecular dynamics.

"Automation of NMR structure determination of proteins", Altieri and Byrd, Curr Opin Struct Biol (2004)

CANDID Protocol

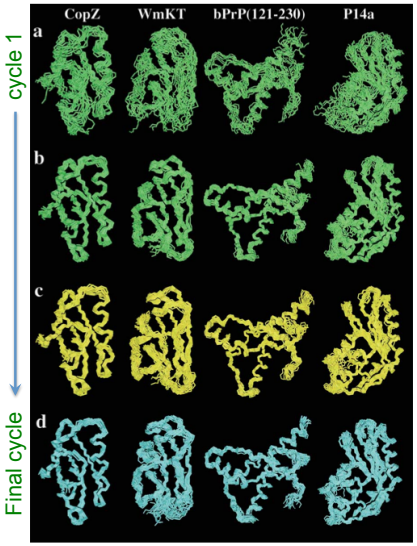

Wuthrich and coworkers, JMB (2002)

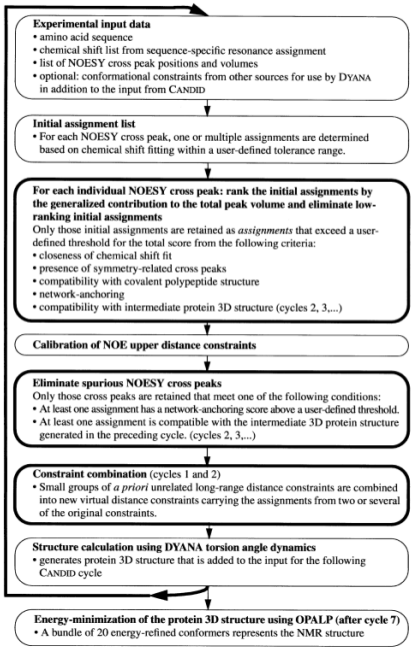

2. Protein Dynamics from Relaxation Analysis

Relaxation parameters (T1, T2, NOE) determined mainly by molecular tumbling and also depends on internal dynamics They thus report on internal dynamics, even though not always in obvious ways!

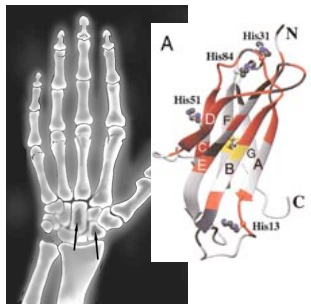

blue: with Cu^{2+}; red: without

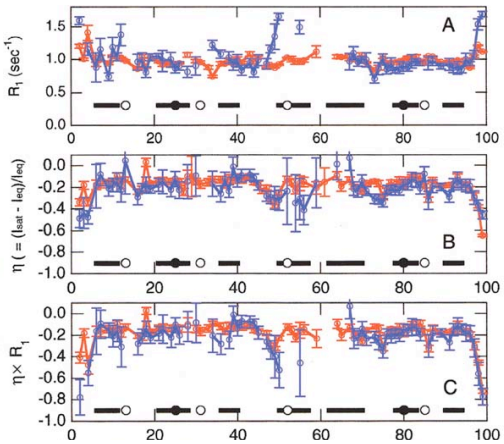

Villanueva et al., "Increase in the conformational flexibility of β_2-microglobulin upon copper binding: A possible role for copper in dialysis-related amyloidosis", Prot. Sci (2009).

Quantitative Analysis of NMR Relaxation

- With (proton-proton) cross-relaxation suppressed, amide N15 relaxes primarily due to dipolar interaction with the directly attached 1H spin and through 15N Chemical Shift Anisotropy.
- Relaxation parameters determined by spectral densities:

$$R_1 = \frac{d^2}{4}[3J(\omega_N) + J(\omega_H - \omega_N) + 6J(\omega_H + \omega_N)] + \frac{c^2}{3}J(\omega_N), \quad (1)$$

$$R_2 = \frac{d^2}{8}[4J(0) + 3J(\omega_N) + J(\omega_H - \omega_N) + 6J(\omega_H) + 6J(\omega_H + \omega_N)] + \frac{c^2}{18}[4J(0) + 3J(\omega_N)] + R_{ex}, \quad (2)$$

$$\mathrm{NOE} = 1 + \frac{d^2}{4R_1}\frac{\gamma_H}{\gamma_N}[6J(\omega_H + \omega_N) - J(\omega_H - \omega_N)], \quad (3)$$

$$d = (\mu_0 h \gamma_H \gamma_N / 8\pi^2) < r_{NH}^{-3} > \text{ and } c = \Delta\sigma\omega_N;$$

r_{NH} is the length of the N-H bond; $\Delta\sigma$ is the CSA of 15N; ω_H and ω_N are the Larmor frequencies of 1H and 15N

Chen et al., JBNMR (2004) and references therein.

Spectral Density and Internal Motions

- The spectral density function is the Fourier transform of the angular auto-correlation function, C(t), of the N-H bond vector,

$$J(\omega) = 2\int_0^\infty C(t)\cos\omega t\, dt.$$

- The auto-correlation function depends on both overall tumbling and internal dynamics. Assuming $C(t) = C_o(t)\, C_I(t)$, if tumbling much slower.
- In so-called "model-free" analysis (Lipari and Szabo, 1982), internal dynamics characterized by (motion) model-free parameters, including
  - generalized order parameters (**S**): amplitudes of the internal motions
  - Effective time constants (τ): time-scales of the internal motions

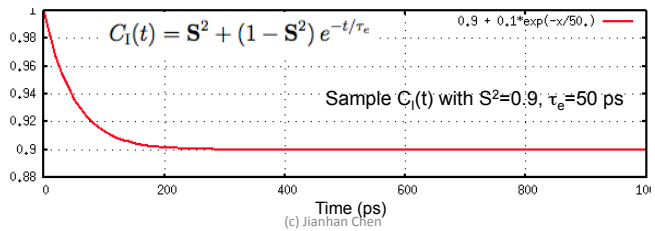

Model-Free Analysis

- Measure T1, T2 & NOE, typically at two fields (e.g., 500 MHz and 600 MHz)
- For each N15, fit (three or six) relaxation data points to to obtain generalized order parameters (S) and effective time constants (τ).
- These dynamics parameters quantify protein internal dynamics and can be use to understand the role of internal dynamics in folding and binding.

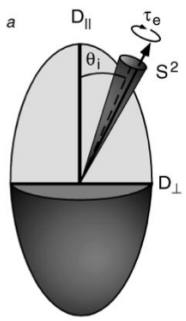

$$J(\omega) = \frac{2}{5}\left[\frac{S^2\tau_m}{1+(\omega\tau_m)^2} + \frac{(1-S_f^2)\tau'_f}{1+(\omega\tau'_f)^2} + \frac{(S_f^2 - S^2)\tau'_s}{1+(\omega\tau'_s)^2}\right] \quad (4)$$

in which $\tau'_f = \tau_f\tau_m/(\tau_f + \tau_m)$, $\tau'_s = \tau_s\tau_m/(\tau_s + \tau_m)$, τ_m is the isotropic rotational correlation time of the molecule, τ_f is the effective correlation time for internal motions on a fast time scale defined by $\tau_f < 100-200$ ps, τ_s is the effective correlation time for internal motions on a slow time scale of ~1 ns defined by $\tau_f < \tau_s < \tau_m$, $S^2 = S_f^2 S_s^2$ is the square of the generalized order parameter characterizing the amplitude

NMR PROBES OF MOLECULAR DYNAMICS: Overview and Comparison with Other Techniques, Palmer, Annu Rev Biophys Biomol Struct (2001).

Assumption of uncoupled tumbling and internal motions in model-free analysis likely leads to an underestimation of motions on ns timescales.

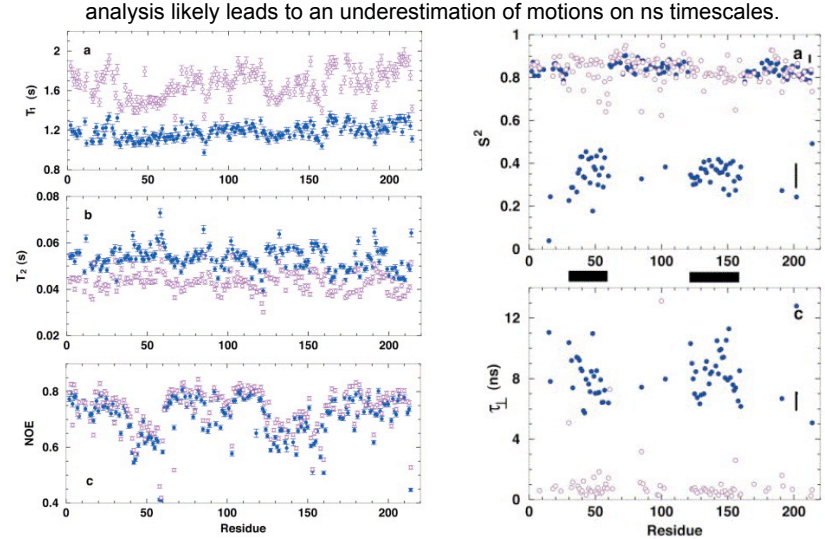

A novel view of domain flexibility in E. coli adenylate kinase based on structural mode-coupling 15N NMR relaxation, Tugarinov et al, JMB (2002).

Protein dynamics in enzyme catalysis

The synergy between structure and dynamics is essential to the function of biological macromolecules. …. Here we show that pico- to nano-second timescale atomic fluctuations in hinge regions of adenylate kinase facilitate the large-scale, slower lid motions that produce a catalytically competent state. The fast, local mobilities differ between a mesophilic and hyperthermophilic adenylate kinase, but are strikingly similar at temperatures at which enzymatic activity and free energy of folding are matched.

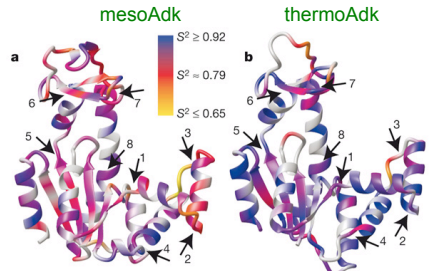

The connection between different timescales and the corresponding amplitudes of motions in adenylate kinase and their linkage to catalytic function is likely to be a general characteristic of protein energy landscapes.

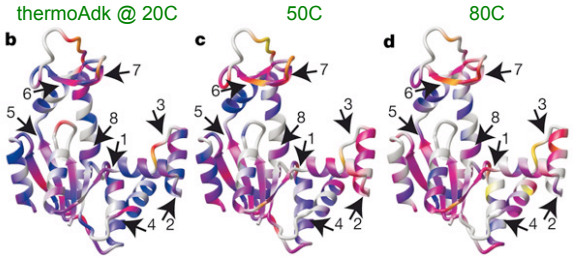

A hierarchy of timescales in protein dynamics is linked to enzyme catalysis, Kern and coworkers, Nature (2007)

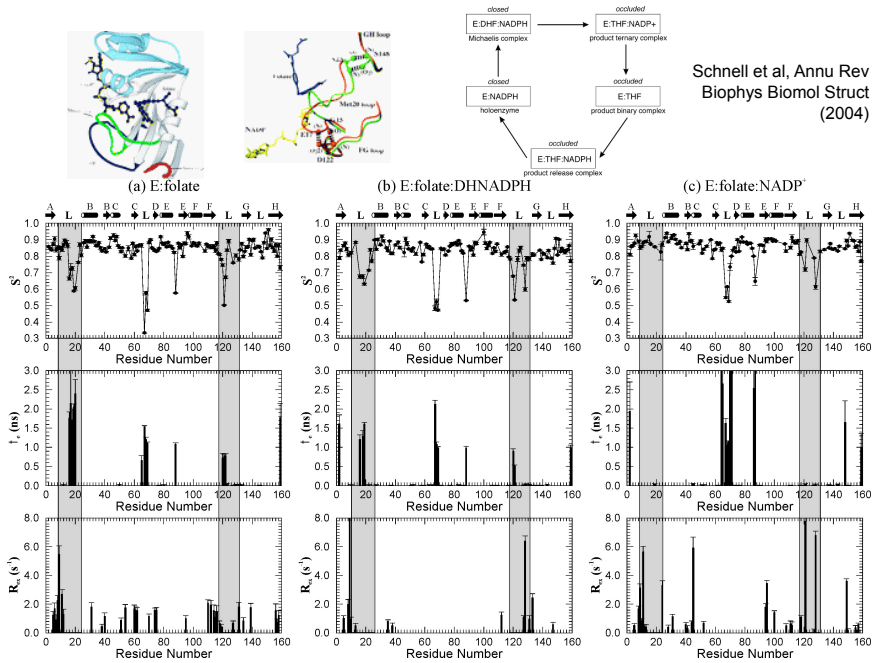

Schnell et al, Annu Rev Biophys Biomol Struct (2004)

Conformational Entropy in Protein Interaction

Here we employ changes in conformational dynamics as a proxy for corresponding changes in conformational entropy. We find that the change in internal dynamics of the protein calmodulin varies significantly on binding a variety of target domains. Surprisingly, the apparent change in the corresponding conformational entropy is linearly related to the change in the overall binding entropy. This indicates that changes in protein conformational entropy can contribute significantly to the free energy of protein–ligand association.

Wand and coworkers, Nature (2001); Nature (2007)

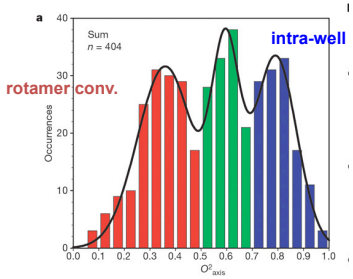

(sidechain methyl axial)

$$\Delta S = k\sum_{\alpha}\ln\left(\frac{1-S_{\alpha 2}^{2}}{1-S_{\alpha 1}^{2}}\right)$$

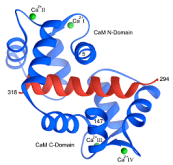

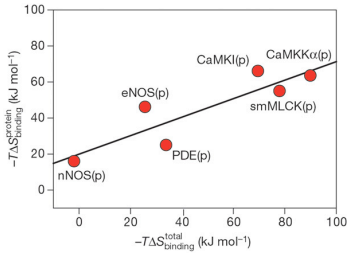

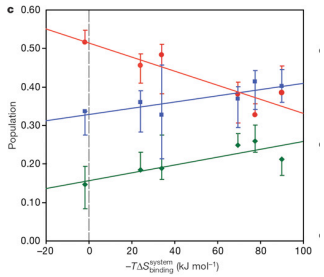

Coupled Binding and Folding

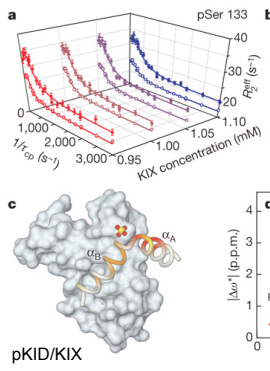

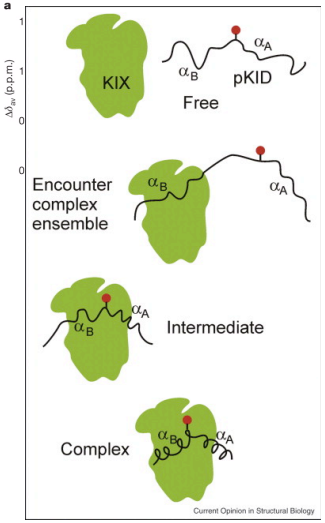

Wright and coworkers, Nature (2007); COSB (2009)

3. Spin-labeling and Transient Interactions

- Paramagnetic centers enhance NMR relaxation, typically undesired.
- Paramagnetic relaxation enhancement (PRE) coupled with site-directed spin-labeling (SDSL), however, provides distance information up to 35 Å.
  - Allows one to detect long-range ordering and transient structures!

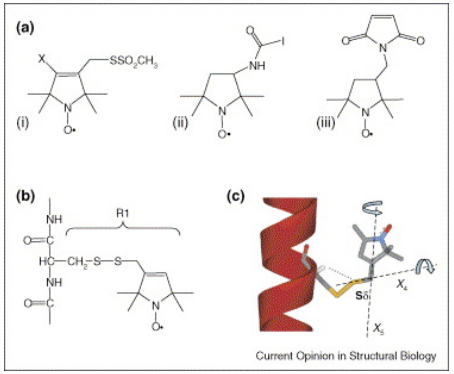

Structures of typical nitroxide-based spin probes

Structural Reorganization of α-Synuclein

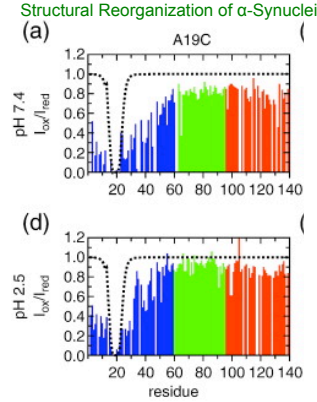

Fanucci & Cafiso, COSB (2006); Wu et al, JMB (2009)

Visualizing transient events in amino-terminal autoprocessing of HIV-1 protease

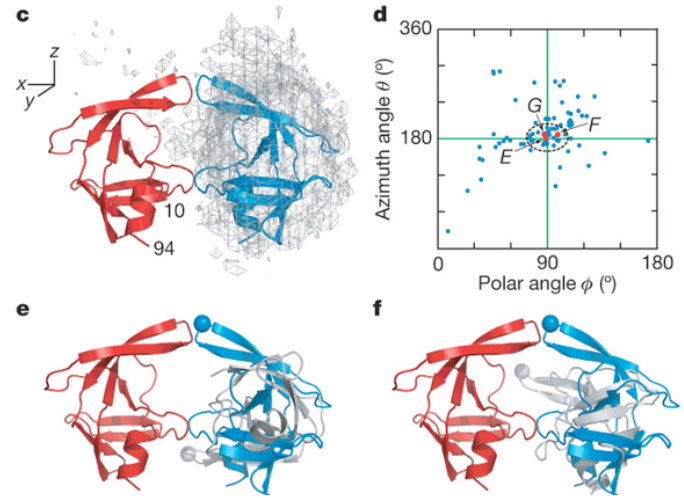

PREs were measured on a 1:1 mixture of 0.2 mM U-[2H/13C/15N]-labelled ^{SFN}FPR(D25N) and spin-labelled ^{SFN}FPR(D25N) at natural isotopic abundance.

Tang et al, Nature (2007)

5. In-Cell NMR

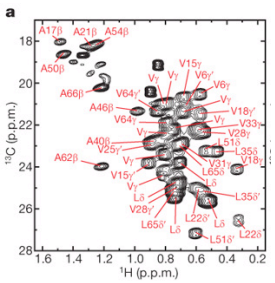

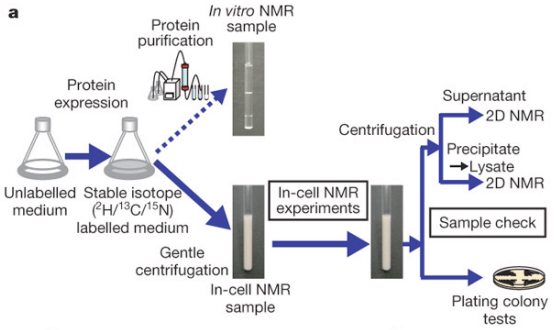

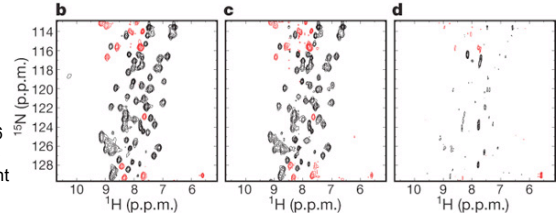

a, Scheme of the in-cell NMR experiments using E. coli cells. b, The 1H–15N HSQC spectrum of a TTHA1718 in-cell NMR sample immediately after sample preparation. c, The 1H–15N HSQC spectrum after 6 h in an NMR tube at 37 °C. d, The 1H–15N HSQC spectrum of the supernatant of the in-cell sample used in b and c.

Protein structure determination in living cells by in-cell NMR spectroscopy, Sakakibara et al, Nature (2009).

A putative heavy-metal binding protein TTHA1718 from Thermus thermophilus HB8 overexpressed in Escherichia coli cells.

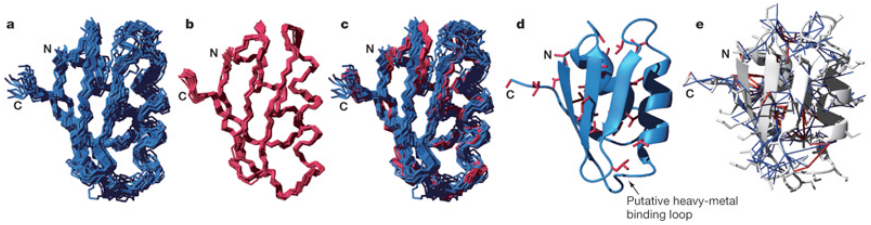

a, A superposition of the 20 final structures of TTHA1718 in living E. coli cells, showing the backbone (N, Calpha, C') atoms. **b**, A superposition of the 20 final structures of purified TTHA1718 in vitro. **c**, A comparison of TTHA1718 structures in living E. coli cells and in vitro. The best fit superposition of backbone (N, Calpha, C') atoms of the two conformational ensembles are shown with the same colour code in a and b. **d**, Secondary structure of TTHA1718 in living E. coli cells. The side chains of Ala, Leu and Val residues, the methyl groups of which were labelled with 1H/13C, are shown in red. **e**, Distance restraints derived from methyl-group-correlated and other NOEs are represented in the ribbon model with red and blue lines, respectively.

Protein structure determination in living cells by in-cell NMR spectroscopy, Sakakibara et al, Nature (2009).

6. MRI

- "magnetic resonance tomography"
- First MR image in 1973
- 2003 Nobel Prize
- Detect T1 or T2 relaxation of water protons in body
- Contrast agent to enhance the contrast (increase the spread of T1/T2 in tissues)
- B_0 ~ 1.5 T (60 MHz)
- Extensive use of magnetic field gradient for plane selection

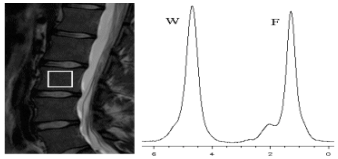

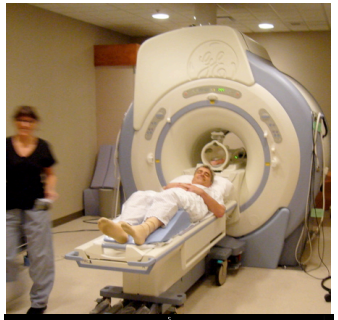

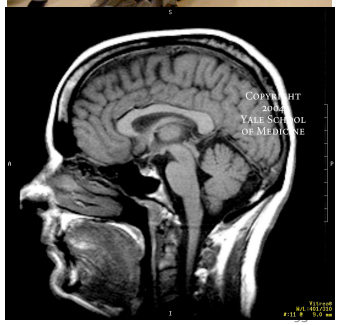

Additional reading: http://www.cis.rit.edu/htbooks/mri/